Chapter - 5 : Sorption and desorption of thionine and its derivatives on and from Na-montmorillonite

CHAPTER - 5

SORPTION AND DESORPTION OF THIONINE AND ITS DERIVATIVES ON AND FROM Na-MONTMORILLONITE

5.1.1 Introduction and Review of previous work

Though investigation of clay minerals may be traced far back into antiquity, the clay mineral concept developed only in the present century with the systematic studies for the origin of the colloidal properties of clay mineral. Considerable success has been achieved in the past fifty years with regard to the search for high purity clays and for evidences of their crystallinity. The "atomic structures" of the common clay minerals have been to a great extent determined and applied to explain the properties of the individual members by numerous investigators.

On the basis of crystal chemical approach, the correlation between the structures and the exchange properties of the clay minerals has established from the important researches of Pauling (107), Bragg (108), Gruner (109), Brindley (110), Hofmann (111), Marshall (112), Hendricks (113) and others (114-120). From these studies, clay minerals are recognised to consist essentially of two structural units. One is composed of two sheets of closely packed oxygens or hydroxyls in which aluminium or magnesium atoms are arranged in octahedral co-ordination so that they are equidistant from six oxygens or hydroxyls. With aluminium in the octahedral

position, only two-thirds of the possible positions are filled to balance the structure. It is the gibbsite structure having the formula $Al_2(OH)_6$. When magnesium is present, all the possible positions are filled up to balance the structure giving the brucite which has the formula $Mg_3(OH)_6$. The second unit is the tetrahedrally co-ordinated silica. A silicon atom being placed at the centre of a regular tetrahedron is equidistant from four oxygens or hydroxyls. The silica tetrahedra are joined together through oxygen, to form a hexagonal net work which is repeated indefinitely for form a sheet of composition $Si_4O_6(OH)_4$. The tips of all the tetrahedra are in the same direction. The structure of aluminosilicate particularly montmorillonite used in the present study is described briefly.

Montmorillonite:

According to the currently accepted concept, montmorillonite is composed of units made of two silica tetrahedral sheets, with a central alumina octahedral sheet. All the tips of the tetrahedra are, pointed in the same direction and toward the centre of the unit. The tetrahedral and the octahedral sheets are combined in such a way that the tips of the tetrahedra of each silica sheet and one of the hydroxyl layers of the octahedral sheet form a common layer. The atoms common to the tetrahedral and octahedral layers become O instead of OH.

The minerals of the group are also developed by stacking of these unit sheets one above the other. During stacking, the O layers of one unit are close to the O layers of the other unit, so that there is an excellent cleavage between the sheets. Polar

molecules can enter into the space between the sheets causing expansion of the interlayer space.

Usually during crystal growth, the tetrahedra are not solely occupied by silicon or by aluminium of magnesium. Aluminium may substitute for some of the tetrahedral silicon atoms and Fe, Li, Mn, Cr and other metal ions of suitable size may occupy a part of the octahedral sites. This isomorphous replacement of ions unbalances the overall charge of the crystal lattice. An excess negative charge develops which is balanced by cations that are retained on the external layer silicate surfaces. These cations e.g. Na^{+}, K^{+}, Ca^{+2} and others are more or less exchangeable, depending on the nature of the replacing cations, nature of the adsorbed cations, and the magnitude and distribution of the structural charge. They are held between unit layers and bind the layers together. This brings the idea of cation exchange capacity (c.e.c) of the clay minerals.

Ion-exchange property of clay minerals:

The ion-exchange sorption of inorganic as well as organic ions is known to occur in clay minerals (121-125). The origins of charge of the clay lattice are believed to be due to lattice imperfections, broken bonds at the edges of the particles and exposed structural hydroxyls in addition to the isomorphous substitution already mentioned. The negative charge on the clay minerals is compensated by adsorption of cations. The counter ions are held on the external surfaces of the aggregates and between the unit layers in clays which swell in aqueous suspension, whereas the sorption of

counter ions takes place onto the external surfaces in non-swelling clays. In aqueous suspensions, some of these cations remain in a closely held Stern layer, others diffuse away from the surface and thus form a diffused double layer. Provided that they are not fixed by engaging in strong, specific bonding with the clay or by being trapped between unit layers that have collapsed together irreversibly (lattice collapse), the counter ions can undergo ion exchange with other cations present in the system. The magnitude of the c.e.c. of a clay depends largely on the type of clay and to a lesser extent on the source of a particular sample.

Besides cation exchange capacity, the specific surface area of a clay mineral is another important property that depends on the type of clay and also on the method of measurement employed. Among clays of the same type, the values differ from sample to sample; the nature of the counter ions present in the same sample may also influence the measured surface area. The theoretical surface areas are calculated from the weights of the unit cells and their dimensions as indicated by X-ray diffraction.

Systematic studies of cation exchange in pure clay minerals were carried out by Page and Baver (126), Bar and Tenderloo (127), Hendricks and Alexander (128), Schachtschabel (129), Mukherjee (130) and others. Most of these investigations were based on exchange equilibria, selectivity etc. with simple inorganic ions (131-132). Exchange reaction involving clay minerals with organic compounds have also been established by different scientists (133-136).

Martin and Glaeser (137) studied the adsorption of $Co(NH_3)_6Cl_3$ on montmorillonite under various pH conditions. They found that it permits the estimation of internal and external exchange capacities. Das Kanungo, Chakravarti and Mukherjee (139-141) studied adsorption and desorption of hexamine cobalt (III) chloride and tris-ethylene diamine cobalt (III) chloride on montmorillonite and vermiculite and observed that adsorption is according to Langmuir's equation and desorbing cations arrange themselves according to the lyotrope series.

Recently, Sarkar and Das Kanungo (142) have shown that in the exchange of tris-trimethyl diamine Co(III) from the bentonite matrix by alkaline earth metal ions, both the hydrated ionic radius and the reciprocal of the Debye-Huckel ion-size parameter, a°, may be used to correlate the relative affinities of the ions for the mineral while for the alkali metal ions only, $1/a^{\circ}$ may be utilised for the purpose.

Interlayer complexes of clays with simple organic compounds are essentially of two types; in one type the adsorbed species exists as a cation and in the other as a polar non ionic compound.

Following up the work on clay mineral-organic complexes that began as early as 1916, Gieseking and co-workers (135,138,143,145) examined the interaction of montmorillonite clays with a number of organic bases, cations and proteins. Hendricks (144) extended this study to other aliphatic and aromatic amines, alkaloids, purines and nucleosides using H-montmorillonite as adsorbent. The chemistry

of clay-organic reaction has been well reviewed by Greenland (146), Mortland (147) and Theng (148). A number of general conclusions has emerged from these studies is summarized below.

(i) Adsorption reaches a maximum equal or close to the exchange capacity of the clay. For very long chain derivatives ($\rangle C_8$), adsorption may exceed this capacity, the excess being present as free molecules.

(ii) For montmorillonite, the affinity of the organic ion for the clay surface increases regularly with molecular weight, that is the larger the cation, the stronger is its adsorption. This is ascribed to the increased contribution of van der Waals forces to the adsorption energy as the molecular weight increases and also to the changes in the hydration status of the ions in the clay interlayer.

(iii) Basal spacing measurements suggest that the organic ion is adsorbed with its shortest axis perpendicular to the silicate layer, since such a flat conformation affords a close van der Waals contact between the adsorbate and substrate.

(iv) Single layer complexes ($d_{001} \simeq 12.5\text{-}13.5\ A^{\circ}$) are formed with montmorillonite provided that the area of the cation (upto C_{10}) is less than the area per exchange site, since the organic ions adsorbed on one layer can fit into the gaps between those adsorbed on the opposing surface. If, however, the cation area ($\rangle C_{10}$) exceeds the area per exchange position, this lock-and-key arrangement is no longer possible and double layer complexes ($d_{001} \simeq 16.5 - 17.5A^{\circ}$) are obtained.

(v) At high surface concentrations, long chain alkylammonium ions ($\rangle C_{10}$) may assume an 'end-on' orientation in which the alkyl chain extends away and makes a definite angle with the silicate surface. In this conformation greater van der Waals interactions between alkyl chains are possible. The interlayer space is also increased so that a larger amount of the organic ions can be accommodated.

(vi) There is evidence to indicate that partially exchanged montmorillonite crystals are composed of "inorganic ion rich" and "alkyl ammonium ion rich" layers as shown by Barrer and Brummer (150) and Theng et al. (149) and others.

Sorption studies of dyes and large organic ions on different adsorbents, particularly on clays, have been made by many workers. Most of the studies have been confined to the measurement of the surface areas and c.e.c. of the adsorbents.

As early as 1910 Mare (151) observed that dyes could be adsorbed by crystals upto a saturation value. Ramchandran et al. (152) measured the surface area by low temperature nitrogen adsorption of methylene blue, methyl violet and malachite green on the clay fraction of montmorillonite, kaolinite and illite. From the difference, the actual extent of the area of contact was evaluated. This was found to be relatively small showing that while the surface is available for nitrogen adsorption, it is not accessible to dye molecules. The cation exchange capacity, found from methylene blue and methyl violet sorption on kaolinite and montmorillonite, was

in close agreement with those found by standard methods.

Brooks (153) adsorbed methylene blue on Na^+ forms (Na^{22} and Na^{23}) of montmorillonite, kaolinite and silica sand flour and found the amount of dye adsorbed to be equivalent to the sodium displaced; he believed that the dyes were adsorbed on the clay mineral surface through ion-exchange process. Plesch and Robertson (154) also proposed two distinct mechanisms to operate in sorption of dyes on surfaces of clay minerals; namely the partly irreversible ion-exchange and the fully reversible physical adsorption. Bergmann and O'Konski (42) reported that the adsorption of methylene blue on montmorillonite took place first through irreversible ion exchange mechanism and then by physical adsorption and verified the equation of Plesch and Robertson with their experimental results.

Ewing and Liu (155) estimated the cross-sectional areas of crystal violet and orange II assuming that the dye molecules were adsorbed flat on the surface of clay minerals and they estimated the cross-sectional area of Crystal violet to be 160 A^{o2} and 171A^{o2} depending on whether the dye is adsorbed in the dehydrated or hydrated condition.

The surface areas measured through dye adsorption, however, did not agree with those obtained by nitrogen adsorption in all cases. Kipling and Wilson (156) found discrepancies in specific surface areas of porous and non-porous active charcoal measured by methylene blue and nitrogen adsorption. Hofmann (157), on the basis of methylene blue and orange II adsorption on a wide variety of clays, showed that the surface area calculated was only 70% of the

total surface area. Orr (158,159) found that the surface areas of two halloysite samples calculated by sorption of four dyes viz. malachite green oxalate, malachite green hydrochloride, amaranth and tetrazine, were apparently equal to 1/4th of the total surface. Similar discrepancies were also reported by Darau (160), van der Grinter (161) and Bancelin (162) in their respective adsorption studies. Bancroff et al. (163) from adsorption of methylene blue on lead sulphate, Subrahmanya et al. (164) from crystal violet adsorption on glass and Doss and Singh (165) from thymol blue adsorption on active carbon, arrived at similar unsatisfactory results.

Giles et al. (166) observed that the adsorption of basic dyes by silica from aqueous solution exceeded its monolayer coverage requirement. Association of the dye molecules in the adsorbed state has also been detected by electron micrography (167). That most of the dye molecules are associated in solution as micelles from 10 to 100 molecular units was reported by Lenhar and Smith (168,169), Vickerstaff and Lemin (170) and Bergmann and O'Konski (42). Mukherjee and Ghosh (35,171,172), Hertz et al. (174) and Hertz (173) also observed that dye molecules, of which the monovalent organocations are a sub group, tend to aggregate into dimeric and polymeric species in aqueous solution. Kongonoviski (175) also viewed the adsorption of dyes to take place through monolayer sorption of associated micelles. Brooks (153) however advocated that the surface area and cation exchange capacity of the substrates, with methylene blue adsorption, could still be measured. To calculate c.e.c. and surface areas, he suggested addition of dye solution to a mineral suspension

in small increments till the equilibrium concentration was $1x10^{-6}$M, indicated by a slight blue colour of the supernatant.

Hang Pham Thi and Brindley (176) asserted that methylene blue can be used for the measurement of both surface areas and c.e.c. of clay mineral such as montmorillonite. They attributed the cause of failures in measuring surface areas and exchange capacities by Faruki et al. (177) and Bodenheimer and Heller (178) to the insufficient replacement of Ca^{+2} ions by methylene blue from Ca-montmorillonite used in their studies. Using Na-clay instead of the Ca-clay these authors calculated surface areas from the amount of methylene blue adsorbed when optimum flocculation occurred. Fully exchanged values of methylene blue was used to calculate the c.e.c. of the montmorillonite. Methylene blue molecule was considered to possess approximately a rectangular volume of dimensions 17.0 x 7.6 x 3.25A^{o3}. They believed that coating of clay particles occurred first and visualised a flat face-on orientation of methylene blue molecules (i.e. lying on the 17.0 x 7.6 A^{o2} face) for effective coverage of surfaces. Flat face-on orientation of the dye (i.e. 17.0 x 3.25A^{o2} face) was assumed when full exchange took place.

West, Carrol and Whitcomb (179) investigated systematically the adsorption characteristics of more than thirty dyes on photographic bromo-iodides or chloro-bromides suspension in 70% aqueous gelatine solution in an attempt to correlate the sorption and optical sensitisation. It was noticed in some cases that the dye adsorbed was very little at first but the rate of increase of dye adsorption increased as more dye was adsorbed. They termed this as "co-operative adsorption". The intermolecular forces between the large dye molecules

are so high that they polymerised when the molecules came closer in the adsorbed state, giving rise to increased adsorption.

De et al. (180-186) made a series of studies on sorption of dyes on to clay minerals and on their desorption from the clay-dye complexes by various inorganic and organic ions. They found Langmuir-type of adsorption isotherms to operate in all cases. Surface area measurement, evaluation of c.e.c., determination of selectivity coefficient and distribution coefficients are the major part of their work. Narine and Guy (187) interacted thionine, methylene blue, new methylene blue, paraquat, diquat with bentonite in dilute aqueous systems. They noted that the dye cations form aggregates on the clay surface and aggregation increases with ionic strength, raising the adsorption capacity by 25%. They also observed that changes in adsorption due to changes in temperature were small and the dyes were irreversibly bound by the clay matrix.

Yamagashi (188) recently studied the effect of alkyl chain length ($-CH_3$ to $C_{14}H_{29}$) for the adsorption of n-alkylated acridine orange cations on Na-montmorillonite. He observed that the length of the aliphatic tail had no appreciable effect on the binding constant and the rate of adsorption.

It appears from the review that the sorption of cationic dyes, although believed to be primarily an ion-exchange process, is rather complicated by many factors such as molecular size, molecular geometry, dye-dye interaction, the surface characteristics of the sorbents. In this context an attempt has been made in the present

investigation to study the sorption and desorption behaviour of a series of methyl substituted cationic dyes viz. Thionine, Azure C (MMT), Azure A (DMT), Azure B (TMT) and methylene blue on and from Na-montmorillonite by various monovalent, bivalent and organic ions of varying size and shape.

5.1.2 Ion Exchange Formulations

A number of approaches, both qualitative and quantitative, have been made to understand the equilibria between an ion exchanger and the ions in solution (189). A review of cation exchange equations as they are being used in soils and in other exchangers has been done by Bolt (190) and Helfferich (191) and their applicability to soils discussed by Babcock (192). Experiments were performed in which the ionic concentrations were varied and the result suggested an exponential relationship between the ions adsorbed (or desorbed) and the concentration of the exchanging ions. Limitations have been tacitly accepted in most mathematical treatments of exchange reactions.

Thus (A) the simultaneous occurrence of both cation and anion exchange reactions in a given system has been considered as a rare case, (B) the exchange capacity varies markedly with the change in pH and the nature of the exchanging ion (C) simple stoichiometric equivalence between the ions taken up and released is generally assumed to be present, deviations are usually explained in terms of simultaneous adsorption and formation of complex ions, and (D) finally the perfect reversibility exists in an exchange process under consideration.

On this basis, various formulations similar to Fruendlich and Langmuir's adsorption equations (isotherms) were proposed. The Fruendlich equation is emperical and can be expressed as

$$\frac{X}{m} = k. C^{1/n} \quad * \qquad (30)$$

where 'X' is the amount of adsorbate taken up by "m" gm of adsorbent, 'k' and 'n' are constants and 'C' is the adsorbate concentration in solution at equilibrium.

Weigner (193) used this equation in 1912. But this equation has two limitations, (i) it does not flatten out at higher values of 'C' as a system of fixed exchange capacity should, and (ii) it shows that the exchange varies with variation of total volume, whereas Weigner (193) showed that the position of equilibrium was independent of volume. Weigner and Jenny (194), however, in 1927, overcome the second objection and modified the equation as

$$\frac{X}{m} = k \left(\frac{C}{a-C} \right)^{1/n} \qquad (31)$$

[a = initial concentration of the adsorbate].

With the variable character of two constants incorporated in this equation, a good agreement is often obtained with experimental data over a limited range. However, Marshall and Gupta (195), has shown that it was superior as regard to k but 1/n varied erratically.

The Langmuir isotherm is based on sound kinetic and thermodynamic principles and was developed to describe the adsorption

---

* k in this equation is different from the heterogeneous rate constant k of Chapter 4.

of gases onto solids. It assumes that only monomolecular adsorption takes place, that adsorption is on localised sites, that there are no interactions between adsorbate molecules and that the heat of adsorption is independent of surface coverage. When V is the equilibrium volume of the gas adsorbed per unit mass of adsorbent at pressure P, then

$$V = \frac{V_m \cdot K.P.}{1 + KP} \qquad (32)$$

where K is a constant dependent on temperature, and V_m is the volume of the gas required to give monolayer coverage of unit mass of adsorbent. When applied to adsorption from solution, this equation takes the form (196)

$$\frac{X}{m} = \frac{(x/m)_{max} \cdot K.C}{1 + K.C} \qquad (33)$$

where 'X' is the amount of the solute adsorbed by mass 'm' of adsorbent, 'C' is the equilibrium solution concentration, 'K' is a constant, and $\left(\frac{X}{m}_{max}\right)$ is the monolayer capacity.

By use of the reciprocal expression, the above equation becomes,

$$\frac{1}{(X/m)} = \frac{1}{K_o (X/m)_{max}} \cdot \frac{1}{C} + \frac{1}{(X/m)_{max}} \qquad (34)$$

A plot of 1/x/m versus 1/C should give a straight line and a slope of $\frac{1}{K(X/m)_{max}}$ when the Langmuir relationship holds good.

A similar type of equation of the Langmuir's with two constants were proposed by Vageler (197-198) as

$$X = \frac{S.a}{a + C} \qquad (35)$$

where X = amount exchange, a = electrolyte added

S and C = constants.

Application of the Langmuir's adsorption equation to cation exchange in soils was initiated by Vageler (197) in 1932. His equation appears to be an erroneous attempt to restate the Langmuir equation in terms of amounts of the cation added to the system rather than its concentration at equilibrium. It may be shown that only when the ratio of the forward and backward rate constants is close to unity such a restatement is acceptable and in all other cases it does not appear to be sound (199).

Aside from Vageler's equation, the original Langmuir equation is in its simplest form useless for cation exchange, as it does not take into consideration the competition between the cationic species. One may, however, introduce this competition effect into the Langmuir equation rather simply by using Kerr's (200) and Gapon's (201) equations as a starting point (190).

The ion exchange formulations are usually based on three theories i.e (i) crystal lattice theory (ii) double layer theory

and (iii) Donan membrance theory (203). The only differences in the various theories are the position and the origin of exchange sites. In all cases, this site is essentially a fixed, non-diffusible ionic grouping capable of forming an electrostatic bond with a small diffusible ion of opposite charge. The case with which this latter ion may be replaced depends on the strength of the bond, which varies in a manner similar to the dissociation of weak and strong electrolytes. The laws governing the exchange of ions in these heterogeneous systems are analogous to the laws governing the solutions of electrolytes.

Jenny (204) envisaged a kinetic condition on the surface and derived from statistical approach the equation below

$$W = \frac{+(S+N) \pm \sqrt{(S+N)^2 - 4SN\left(1 - \frac{\gamma_W}{\gamma_b}\right)}}{2\left(1 - \frac{\gamma_W}{\gamma_b}\right)} \quad \ldots \quad (36)$$

where W = number of cations exchanged at equilibrium

N = number of cations added initially

S = saturation capacity

and W, b = constants for each ion.

For similar exchange properties of the two exchanging ions, the above equation reduces to

$$W = \frac{SN}{S + N} \quad \ldots \quad (37)$$

which is quite similar to that of Vageler (9,10).

A more refined approach was introduced by Davis (205,206) and applied to exchange on soil clays by Krishnamoorty and Overstreet (207). Davis considered the probability of replacement of cations with different valency on a regular array of negative point charges as supposed to be present on the exchanger surface.

The first use of the law of mass action in formulating ion exchange as a completely reversible reaction was made by Gansen (208) and Kerr (200), investigating specific mass action equations for uni-univalent and uni-bivalent exchangers as

$$\bar{Y} + X^{+} \rightleftharpoons Y^{+} + \bar{X} \qquad\qquad 2\bar{Y} + X^{2+} \rightleftharpoons \bar{X} + 2Y^{+}$$

$$K_1 = \frac{[\bar{X}][Y^{+}]}{[\bar{Y}][X^{+}]} \qquad K_2 = \frac{[\bar{X}][Y^{+}]^2}{[\bar{Y}]^2[X^{2+}]} \qquad \cdots \quad (38)$$

The bar indicates the ion in the exchanger phase. The constants K_1 and K_2 are termed as selectivity coefficients. The ionic terms represent equilibrium concentration in solution. But owing to the lack of knowledge about the activities of the ionic species in the exchanger phase, the quilibrium constant could only be evaluated qualitatively or emperically. Bauman (209) and Gregor (210) pointed out the difficulties in terms of swelling and volume change particularly of the resins. The model introduced by Gregor (210) although thermodynamically less well-established, bring out clearly the physical action of the swelling pressure. A more rigorous application

of the law of mass action has been made by Boyd and co-workers (211) in which the "solid solution" idea of Vanselow (212) has been the basis on the assumption that the ion exchange is a "solid solution" process. Vanselow visualizing the monolayer as an ideal two dimensional solid solution, assumes the activities of two exchanger components to be proportional to their respective mole-fractions.

In the above formulations, all the exchange sites were assumed to be of equal value. Doubts regarding this were first clearly expressed by Weigner (213) and his co-workers. In order to explain some of their experimental data, they postulated the existence of loosely and firmly bound ions on the surface of the same exchanger. Without the necessary information regarding the surface characteristics of the silicates which Weigner used for this work, he had to invoke the idea of the existence of micropores, edges and cleavages. A remark should be made here on the assumed reversibility of the exchange reaction. There is evidence that certain exchange reactions are incompletely reversible. The obvious example of such a system is the adsorption of potassium by certain clay minerals. The steric factors influence the relative affinity of the clay for different cations, which necessitates the recognition of a range of sites with different relative affinity (214-215). The fact that often the cationic composition in turn influences these steric factors (by a varying degree of collapse of the crystal lattice) suggests a considerable degree of hysteresis in exchange reaction involving inter-lattice sites.

Attempts to understand ion exchange reactions on the basis of electrical double layer, as postulated by Mukherjee (216) yields

no doubt qualitative results but the concept in many respects, conforms better with observations. He assumed two categories of exchangeable ions, the osmotically active ions which constitute the mobile part of the double layer and osmotically inactive ones constituting the immobile part of the double layer. The relationship of crystalline structure of clays with their electrochemical properties and ion exchange characteristics has been studied with fundamental details by Mukherjee and Mitra (217), Mitra and Bagchi (218), Ganguli and Mukherjee (219) and Chakravarti (220).

However, in a more detailed study of the exchange behaviour of soil materials, the monolayer model equations do not offer much perspective for interpretative usage. One should then rather use, the thermodynamic method of presentation as suggested by Gaines and Thomas (221,222). The most promising model for the description of adsorption on external surfaces appears, however, to be a Stern-Gouy double layer approach along with lines as used for the homovalent case by Heald et al. (223) and further advanced by Shainberg and Kemper (224,225). Extension of this model to heterovalent exchange will increase its complexity considerably, as both the fraction of the multivalent ions in the Gouy layer and that in the Stern layer will depend on the valency. The contribution of Shainberg and Kemper (224,225) is of great interest as an effect to estimate the magnitude of the pair - formation constants on the basis of the physical properties of the ions and presents an important stepforward in the process of gaining understanding about the nature of the cation exchange equilibrium in clay systems.

Considerable progress has also been made by others (226-228) in the formulation of ion exchange equilibria on a rigorous and quantitative basis. Further progress must await new advances in the fields of concentrated solutions of simple electrolytes and soluble, uncrosslinked polyelectrolyte solutions which has been stepped by Fuoss (229), Katchaesky (230) and others.

In the present chapter, an attempt has been made to fit the adsorption data of five progressively alkylated thiazine dyes viz. Thionine, Azure C, Azure A, Azure B and Methylene blue on Na-montmorillonite, in the Langmuir equation and the desorption data of these dyes from their respective adsorbent complexes by monovalent and bivalent inorganic ions and organic ions in the model of Pauley (231).

Pauley's Model:

Pauley has interpreted selectivities in ion exchange equilibrium in the language of a very simple model. Its essential feature is the electrostatic attraction between the counter ions and the fixed ionic groups. It is assumed that all the counter ions in the ion exchanger are found at their distance of closest approach to the fixed ionic groups. Writing AR and BR for the pairs of fixed ionic groups and counter ions at the distance of closest approach, one can split the exchange of A for B into two processes:

$$AR \longrightarrow A + R \qquad \ldots (39)$$

$$R + B \longrightarrow BR \qquad \ldots (40)$$

Coulomb's law (without any correction) leads to the following results for the above processes.

$$\Delta G_1^\circ = \int_{a_A^\circ}^{\infty} \frac{e^2}{r^2 \epsilon} dr = \frac{e^2}{a_A^\circ \epsilon} \quad \cdots \cdots \cdots (41)$$

and

$$\Delta G_2^\circ = \int_{\infty}^{a_B^\circ} \frac{e^2}{r^2 \epsilon} dr = -\frac{e^2}{a_B^\circ \epsilon} \quad \cdots \cdots \cdots (42)$$

where G_1° and G_2° are the free energy changes for the processes 39 and 40, e = electronic charge, ϵ = dielectric constant, r = distance from the centre of the fixed charge, a_i° = distance of the closest approach between counter ion 'i' and fixed ionic group. Hence the overall free energy change for the whole process is

$$\Delta G^\circ = \Delta G_1^\circ + \Delta G_2^\circ = \frac{e^2}{\epsilon} \left(\frac{1}{a_A^\circ} - \frac{1}{a_B^\circ} \right) \quad \cdots \cdots (43)$$

and the thermodynamic equilibrium constant K_A^B is

$$\ln K_A^B = -\frac{\Delta G^\circ}{kT} = \frac{e^2}{kT\epsilon} \left(\frac{1}{a_B^\circ} - \frac{1}{a_A^\circ} \right) \quad \cdots \cdots (44)$$

In the exchange of various univalent counterions 'i' for an arbitrary univalent reference ion A, a linear relationship should exist between $\ln K_A^B$ and $\frac{1}{a_i^o}$.

For multivalent ions, the calculation is not quite as simple because assumptions must be made as to how the (univalent) fixed ionic groups and polyvalent counterions are paired. The model leads qualitatively to preference of the ion exchanger for counterion with smaller a^o value and higher valency.

5.1.3 Exchange studies and Selectivities of Clay minerals

A true ion-exchange equilibrium is completely reversible and may be approached from both sides of the reaction equilibrium provided that certain conditions are observed. These conditions are determined by the selectivity of the ion exchanger which in turn is influenced by Donnan effects, specific interactions, steric effects, ion association and other ion-sequestering effects (202). Where these effects are large the equilibrium will favour one side of the reaction. Specific interactions and Donnan effects largely determine ion selectivity in most situations. Specific interactions (e.g. hydrogen bonding, van der Waals forces, charge-transfer processes, etc.) can produce secondary adsorption interactions on the counterion bound by the exchanger. These increase the selectivity of the adsorbent for the adsorbed ion, and this ion is then held preferentially despite the presence of high concentrations of counterions in solution (191, 232,233). Steric effects can also influence reversibility, as evidenced in ion trapping effects. In some systems ion-sequestering effects (including ion-pairing, complexing and precipitation) are important in determining selectivity. Generally the adsorbent prefers the ion which associates least strongly in solution and most strongly with the adsorbent (191). A number of workers have thoroughly investigated the exchange properties of the clay minerals, resins and molecular sieves and their characteristics have been well established. The following generalisations may be made regarding the tendency of a cation to exchange onto a negative surface. There is an increase in exchangeability (a) with decreasing hydrated ionic radius and increasing polarizability, (b) with decreasing ease of

cation hydration and (c) with increasing counterion charge.

The above criteria, however, do not hold good in cases where some specific interactions take place. In accordance with the above observations, the order of increasing preference of alkali metal ions for ion exchange onto montmorillonite (234-255), is $Li^+ < Na^+ < K^+ < Rb^+ < Cs^+$. The exchange of NH_4^+ is complicated by physical adsorption of ammonia (256) and fixation of NH_4^+ ion (257). It was observed that NH_4^+ is held strongly than Na^+ (258) or even Rb^+ (259).

Similarly, the exchange of H^+ is also complicated due to its attack onto clay lattice, displacing aluminium or magnesium ions which may be taken up by the exchange sites (260, 261). It was reported that H^+ is apparently preferred over some divalent cations in ion exchange on montmorillonite and soil-clays (242,255). The reported relative orders of exchange on montmorillonite are $H^+ < Cs^+$ (245), $K^+ < H^+ < Ca^{2+}$ (236) and $K^+ < NH_4^+ < H^+ < Mg^{2+}$ (263). Under conditions which minimise dissolution of clay by acid attack, the corresponding orders were $H^+ < Na^+ < K^+$ (239) and $Na^+ < H^+ < NH_4^+$ (258). The sequence of exchange of alkaline earth ions on clays has generally been reported as $Mg^{2+} < Mn^{2+} < Ca^{2+} < Sr^{2+} < Ba^{2+}$ (239, 242, 264-274). For the exchange of divalent transition metal cations on clays, the reported orders of preference are $Mn^{2+} \simeq Ni^{2+} \simeq Fe^{2+} < Co^{2+} < Zn^{2+} < Cu^{2+}$ (275), $Ca^{2+} < Co(II)^{2+}$ (276) and $Ni^{2+} < Ba^{2+}$ (273). A generalisation may be made from studies comparing the exchange of mono, di and trivalent cations on clays that there is a preference for cations of higher charge (236,240,242,245,246,262,263,266,270-272,276-281) although there is exception to this trend. In the usual

general purpose cation exchangers, the selectivity sequence of the most common cations is $Ba^{2+} > Pb^{2+} > Sr^{2+} > Ca^{2+} > Ni^{2+} > Cd^{2+} > Cu^{2+} > Co^{2+} > Zn^{2+} > Mg^{2+} > UO_2^{2+} > Tl^{+} > Ag^{+} > Cs^{+} > Rb^{+} > K^{+} > NH_4^{+} > Na^{+} > Li^{+}$ (282-285).

Under suitable conditions, most organic cations are capable of replacing the interlayer inorganic cations, occupying exchange sites in montmorillonite, vermiculite and illite minerals.

The exchange reaction is stoicheiometric except for some bulky cations when a cover-up effect (144) may operate. Studies on the replacement of exchangeable sodium and calcium from montmorillonite by various alkyl ammonium cations were made by Theng et al. (149). They found that the affinity of the clay for the organic cations was linearly related to molecular weight with the exception of the smaller methyl ammonium and large quaternary ammonium ions. Thus, the more the length of the alkyl ammonium chain increases, the greater is the contribution of physical, non-coulombic forces to adsorption. Within a group of primary, secondary and tertiary amines, the affinity of the alkyl ammonium ions for the clay decreased in the series $R_3NH^{+} > R_2NH_2^{+} > RNH_3^{+}$. These differences were explained in terms of size and shape of the ions. Theng et al. also noted that Na^{+} was much more easily exchanged by the alkyl ammonium ions than was Ca^{2+}. In studies in which the alkyl ammonium ion is replaced by metal cations, Mortland and Barake (286) showed that the order of effectiveness in replacing ethylammonium ion was $Al^{3+} > Ca^{2+} > Li^{2+}$. Furthermore, X-ray diffraction studies on partially exchanged systems

revealed that the organic and inorganic cations were not distributed uniformly throughout all the surfaces of montmorillonite, but that a segregation of the two kinds of ions took place in various layers. This suggests that when the displacement of ethylammonium ion by the metal ion from one interlamellar position begins, it is completed before ethylammonium ions from other layers are exchanged. Similar observations have been reported by Barrer and Brummer (150), McBride and Mortland (287) and Theng et al. (149). The exchange of various alkylammonium cations from aqueous solution by Na-Laponite has been carried out by Vansant and Peeters (288). They observed that the affinity of these organic cations was linearly related to molecular weight, molecular size or chain length of the alkylammonium ions. The affinity sequence has been attributed to the increasing contribution of van der Waals force to adsorption energy as the size of the ions increases (146) and also to the change in hydration state of the ions in the clay interlayer (149,289).

Charge density of the clay mineral may also affect the orientation of adsorbed organic cations through steric effects. Thus, Serratosa (290) showed by infra red absoprtion technique that in Pyridinium montmorillonite, the organic cation assumed an orientation where the plane of the Pyridine ring was parallel with the platelets of the clay mineral and a resulting d_{001} spacing of 12.5A°. On the other hand, pyridinium-vermiculite has the pyridinium cations verticially positioned with respect to the clay platelets and a d_{001} spacing of 13.8A°. Apparently, the close proximity of the cation exchange sites one to another prevents the pyridinium ring from

assuming the parallel position because of the restricted area permitted for each pyridinium unit. When neutral but polar organic molecules are bound to the clay surface by other mechanisms, such as ion-dipole interaction, charge density would also be expected to affect their orientation within the interlamellar regions of swelling clay minerals. It is apparent from the review above that the exchange properties of clay minerals have been thoroughly studied by a number of workers and their characteristics have been well established. The more important characteristics are:

(i) The observations of the lyotropic series though exceptions are often observed.

(ii) Obedience to the Langmuir equation of the data on exchange sorption of large organic molecules (specially the dye molecules). A simple equivalent fraction exchange equation has been proposed to fit in the exchange data of Na^+, K^+, Cs^{2+} on bentonite (291) at 0.5(M) and 1.0(M) external salt concentration.

(iii) Formulation of selectivity coefficient : Exchange measurements can be written in a general way as follows:

$$\frac{1}{Z_1}\bar{A} + \frac{1}{Z_2}B \rightleftharpoons \frac{1}{Z_1}A + \frac{1}{Z_2}\bar{B}$$

Where the bar denotes the species in the adsorbed phase and Z_1, Z_2 and the valencies of A and B respectively.

From the above equation, the selectivity coefficient is expressed as follows:

$$K_A^B = \frac{[A]^{1/z_1}\ [\bar{B}]^{1/z_2}}{[\bar{A}]^{1/z_1}\ [B]^{1/z_2}} \quad \ldots \quad \ldots \quad \ldots (45)$$

The measurement of selectivity coefficient and the obedience of Langmuir's equation are not, however, exclusive of one another.

All these studies are confined to the replacement of one inorganic cation for another. There is very little work on exchange reactions involving two organic cations. The exchange of a large organic cation for another organic cation on montmorillonite had been reported by McAtee (292). Since the organo-montmorillonite is organophilic and hydrophobic, the exchange was carried out in an isooctane isopropyl alcohol mixture. It was found that under the condition of the experiment upto 16 per cent of dimethylbenzyllauryl ammonium cation can be replaced from montmorillonite with dimethyl-dioctadecyl ammonium cation. De, Das Kanungo and Chakravarti (181, 184-186) have shown that cationic dyes e.g. methylene blue, crystal violet, and malachite green adsorbed onto bentonite, vermiculite, kaolinite and asbestos can be exchanged by long-chain surface active ions like cetyltrimethyl ammonium and cetyl pyridinium ions. In the present work desorption of five cationic dyes viz. Thionine, Azure C (AMT), Azure A (DMT), Azure B (TMT) and Methylene blue has been studied with tetraalkyl ammonium ion and long chain surface active ions of varying size and shape.

5.2 EXPERIMENTAL

Adsorption and desorption experiments involving five progressively alkylated thiazine dyes viz. Thionine, Azure C, Azure A, Azure B and Methylene blue and montmorillonite were carried out in order to understand the nature of interaction of these dyes with the montmorillonite sample. Various characteristics of dyes, their structure and method of purification are presented in Chapter-3. The characteristics of the montmorillonite sample used in the present experiment is described below.

Sample	Description	Cation exchange capacity meq/100 gm	Source
1. Montmorillonite	Light grey powder	80*	Evans Medical Ltd., Liverpool, England

* Determined by $BaCl_2$ - $Ba(OH)_2$ method.

The clay fractions of montmorillonite clay mineral having particle size less than 2 mμ were isolated by the usual method of dispersion and sedimentation. The fractions so collected were then treated several times with dilute HCl, and after removal of acid, warmed with 6% H_2O_2 in a water bath to remove trace of any organic matter present. Excess H_2O_2 was decomposed by heating the samples in a water bath. The iron present in the clay minerals was then removed by treating the clay sample with sodium metabisulphite and sodium dithionite in acetate-buffer solution at 60°C followed by centri-

fugation, washing etc. as recommended by Bromfield (293). Finally the clay residues were washed to dispersion and dialysed.

Preparation of Na-Montmorillonite

The clay suspension was converted into Na-form by stirring an approximately 2 per cent suspension of the clay minerals with ion exchange resin (DOWEX 50W x 8) in the Na-form for about four hours. The process was repeated once again to ensure complete conversion of the clay mineral to Na-form. Na-clay (pH 7) so formed were used for adsorption and desorption studies.

Adsorption Studies:

10 ml. portions of the suspensions of known clay content, were pipetted into separate stoppered polypropylene bottles (112) and dye solution of known concentration was added in increasing amount. The total volume was made up to 20 ml by adding the necessary amount of distilled water.

The bottles, with their contents, were shaken for three hours and allowed to stand for at least 24 hours to attain exchange equilibrium. Experiments with several days equilibriation produced the same results indicating that 24 hours were sufficient for attaining equilibrium. The resulting exchanged clays were then centrifuged (10,000 r.p.m.) for 10 minutes and the supernatant liquids were analysed spectrophotometrically. From the difference between the initial concentration and the equilibrium concentration, the amount adsorbed was determined. All operations were carried out at constant room temperature.

The clay content of the suspension is measured by evaporating a known volume of the clay suspension to dryness at 100°C to 105°C in an air oven. The content expressed in g/100 ml are given below

Sample	Clay content in g/100 ml
Na-montmorillonite	1.09

Desorption Studies:

For studying desorption, the clay mineral suspensions are mixed with dye solution and the mixtures are shaken for four hours and allowed to equilibrate overnight at constant temperatures. The excess dye is washed off with distilled water by repeated centifugation of the clay-dye complex till the leachate gave zero optical density. The resulting clay-dye complex is then resuspended in distilled water and used for desorption studies. The percentages of the colloid contents of the suspensions are determined by drying a known amount of each at 100°C to constant weights and are given in table 22.

For the purpose of desorption studies, 10 ml. portions of the suspension are taken in a number of stoppered polypropylene bottles and varying amounts of different electrolytes are added. The total volumes are adjusted to 10 ml by adding requisite amounts

of distilled water. The bottles, with their contents, are shaken for four hours and kept overnight to equilibrate. Preliminary studies showed that this period is sufficient for the purpose. The mixtures are then centrifuged (10,000 r.p.m) for 15 minutes and the dye content of the clear centrifugate is estimated spectrophotometrically.

Table - 22

Sample	Content g/100 ml *
1. Na-montmorillonite - Th	0.119
2. Na-montmorillonite - MMT	0.123
3. Na-montmorillonite-DMT	0.125
4. Na-montmorillonite -TMT	0.128
5. Na-montmorillonite-MB	0.135

* The clay content is different for each sample. It is known however, that the difference does not affect the exchange reactions to a great extent (294).

Of the various electrolytes used in the desorption studies, LiCl, NaCl, KCl, NH_4Cl, RbCl and CsCl are from E. Merck, Germany, Cetyl pyridinium Bromide (CpBr), Cetyl Trimethyl ammonium bromide (CTMABr) are from BDH. Standard solution of these electrolytes are prepared by direct weighing of vacuum dried salts. Tetramethyl ammonium bromide (TMABr), tetra ethyl ammonium bromide (TEABr), tetrapropyl ammonium bromide (TPABr) are all of "Fluka". These are standardized by titration with $AgNO_3$ of E. Merck quality using

K_2CrO_4 as indicator. $MgCl_2$ and $CaCl_2$ solutions are prepared with BDH-AR grade samples and standardized by EDTA titration, using Eriochrome Black-T as indicator and the concentration of $SrCl_2$ and $BaCl_2$ prepared with A.R grade samples are determined by precipitating as sulphates.

Measurement of Concentration of the Dyes:

Quantity of adsorbed or exchanged dyes onto a clay from an aqueous solution is measured by determining with Graphicord, Model No. UV-240, double beam UV-VIS Spectrophotometer (SHIMADZU, JAPAN) using cell of 1 cm path in the visible region. In case of dimerization of the dyes (Bergman and O'Konski, 1963) at higher concentration, this measurement will be complicated. Beer's law is found through trial run to be applicable within 5% error at concentration below 6×10^{-6}(M), for the series of alkylated dyes. The measurements are made at wave lengths which showed maximum absorption (λ_{max} peaks) which are 598 nm for Th, 616 nm for MMT, 633 nm for DMT, 648 nm for TMT and 661 nm for MB.

Salt effects are found for electrolyte concentrations above 0.6(M). The adsorption of these dyes by glass is another possible source of error. Hence the following measures are considered in carrying out adsorption and desorption studies of dyes.

(1) Polypropylene containers are used all along in carrying out the various experiments (112).

(2) The readings in spectrophotometer are taken always after adequate dilution of the experimental solutions.

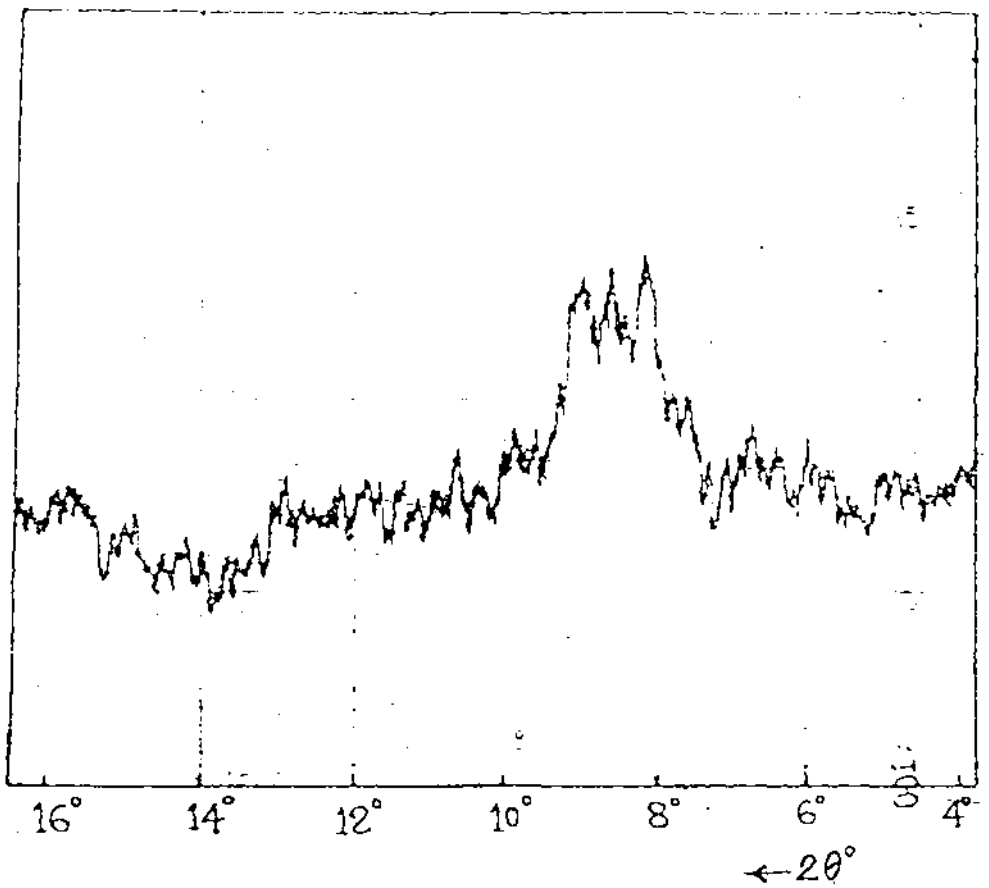

Fig. 76 x-ray diffraction spectra of Na-Montmorillonite .

5.3 Results and Discussion

Due to high exchange capacity and other interesting surface properties, clay modified electrode has been constructed with montmorillonite (Chapter - 4) and as such, the work concerning sorption and desorption on clay minerals have been performed with montmorillonite. The uptake of a large amount of gases by montmorillonite-organic-derivatives, due to the opening of their interlamellar spacings, has been shown by Barrer and his co-workers (295). The sedimentation volume and Zete-potential measurements by Chakravarti (296) have shown that the maximum sedimentation volumes of Aquagel (montmorillonite) recorded by addition of quarternary ammonium salts, is obtained when the salt added is 75 to 80% of the base exchange capacity of the clay. Organic derivatives of montmorillonite exhibit organophilic characteristics and also water proofness, as observed by uptake of toluene/water (297). In the context of the interaction with the organic substances the sorption and desorption characteristics of large dye molecules on and from the surface of montmorillonite are likely to be of interest.

The sorption and desorption characteristics of thionine and its four derivatives on and from Na-montmorillonite are discussed below.

The characteristics of sorption are presented in Section 5.3.1 and those of desorption in Section 5.3.2. The experimental procedures for the studies of sorption and desorption have been described earlier (Section 5.2). The clay used for this study was essentially pure montmorillonite as confirmed by X-ray diffraction analysis (Fig. 76).

5.3.1 Studies On Sorption

Sorption of Thionine on Na-montmorillonite at pH 7:

The adsorption isotherm of thionine on Na-montmorillonite at pH 7, and the corresponding reciprocal Langmuir plot are shown in Fig. 77. The isotherm is of the H-type or high affinity class of Giles et al. (298) and is indicative of species adsorbed flat on the surface. An H-type curve is a special case of the L-type, caused by a very high solute/substrate interaction. The adsorption data are seen to fit into the linear form of the Langmuir adsorption equation. Accordingly, the plot of C/χ vs. C where C is the equilibrium concentration of thionine and χ is the amount adsorbed in meq. per 100 gm of Na-clay, yields a good straight line (Fig. 77b). From the slope of the line, the value of χ_m (the amount required to form a complete monolayer) is found to be 125.8 meq/100 gm, as against the c.e.c of montmorillonite 80 meq/100g. The maximum amount of the dye adsorbed corresponding to the flat portion of the isotherm is 123 meq/100 gm. The excess uptake may be explained by assuming multilayer formation of the adsorbed dye molecules due to dye-dye interaction and sorption of aggregated cations (42), on to the montmorillonite surfaces. Intercalation of dye molecules may also be taken into account for the sorption beyond c.e.c. A similar observation was made by De et al. (299) in their work on methylene blue, crystal violet and malachite green. It is believed that the adsorption is mostly due to ionic and vander Waals forces upto the cation exchange capacity of the mineral and due solely to vander Waals forces beyond it.

The calculated Langmuir bonding constants of thionine obtained from the slope and intercept of the linear plot is equal to 4.00 x $10^5 M^{-1}$. It should be pointed out that when adsorption is in excess of c.e.c. due to sorption of aggregated dye species, the original meaning of the calculated x_m and the Langmuir bonding constant is somewhat altered. Nevertheless, the later parameter still gives some idea about the relative bonding strengths of adsorbents sorbed onto a particular substrate.

The sorption of dye molecules at low concentrations is almost complete, a strong adsorption of Th-cations by Na-montmorillonite being thus indicated.

Sorption of azure C (MMT), azure A (DMT), azure B (TMT) and methylene blue at pH 7:

The adsorption isotherms of thionine derivatives are like that of thionine adsorption, and are initially sharp due to strong affinity of the dye for the montmorillonite surface (Fig. 78-81).

The values of x_m and bonding constants of all the dyes are given below:

Dye-Montmorillonite System	Value of x_m	Value of Bonding Constant
1. Thionine Na-montmorillonite	125.8	4.00 x $10^5 M^{-1}$
2. MMT-Na-montmorillonite	111.0	5.0 x $10^5 M^{-1}$
3. DMT-Na-montmorillonite	95.2	5.25 x $10^5 M^{-1}$
4. TMT-Na-montmorillonite	86.9	5.753 x $10^5 M^{-1}$
5. MB-Na-montmorillonite	86.5	5.875 x $10^5 M^{-1}$

It has been noticed earlier that the c.e.c of Na-montmorillonite is 80 meq/100 gm. while the maximum adsorption of Th, MMT, DMT, TMT and MB onto the clay at 1.4×10^{-4}M equilibrium concentration of the dyes are 123, 106, 94, 85, 85.5 meq/100 gm respectively, which (from figs. 78a, 79a, 80a, 81a) are in the reverse order of their molecular sizes. This may be attributed to the shape and size of organic dye molecules resulting from the difference of alkyl substituents in these dyes. The bonding constant values however, give the usual trend i.e. it increases from thionine to methylene blue which may be attributed to the increase in hydrophobic and vander Waals forces.

The monomer-dimer association constant of thionine, MMT, DMT, TMT and methylene blue in aqueous medium are determined as 1.149×10^3, 1.483×10^3, 2.325×10^3, 3.426×10^3 and 3.574×10^3 respectively at 30°C (discussed in Chapter - 3). It is thus expected that when adsorption takes place from their solutions, MB should be sorbed with larger fraction of the aggregates than that of thionine. As such, the expected order of maximum adsorption would follow the order of their dimerization constant. But interestingly, the order of maximum adsorption (also α_m) is found to be just reversed. It seems apparent that increase in steric hindrance, during interaction of dyes with montmorillonite, from thionine to methylene blue is responsible for above behaviour. In addition, due to flat orientation on clay surfaces, larger dye molecules may cover up some of the exchange sites more effectively making those sites unavailable for further adsorption.

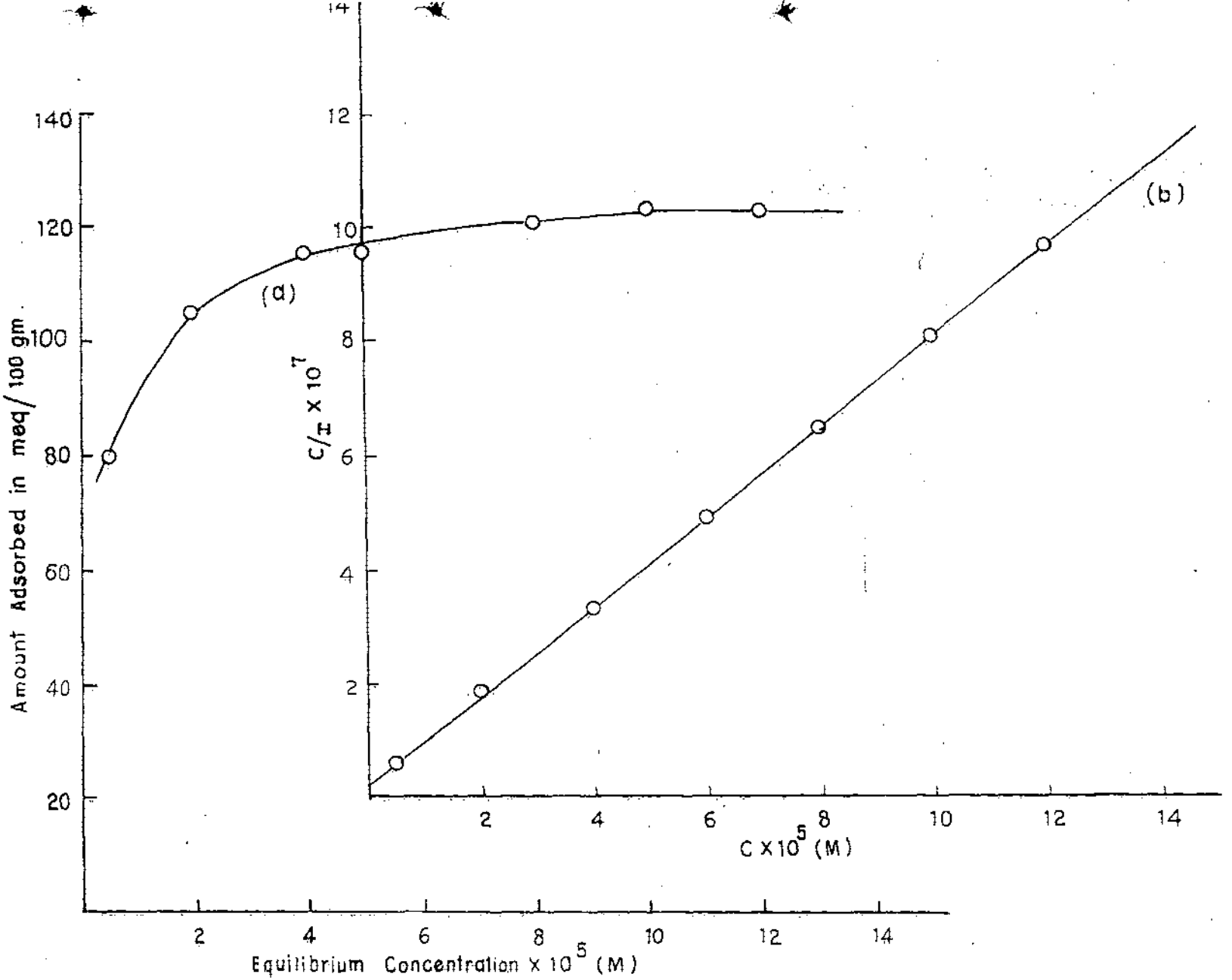

FIG. 77 ADSORPTION ISOTHERM AT 27°C (a) AND LANGMUIR PLOT (b) OF THIONINE ON Na-MONTMORILLONITE.

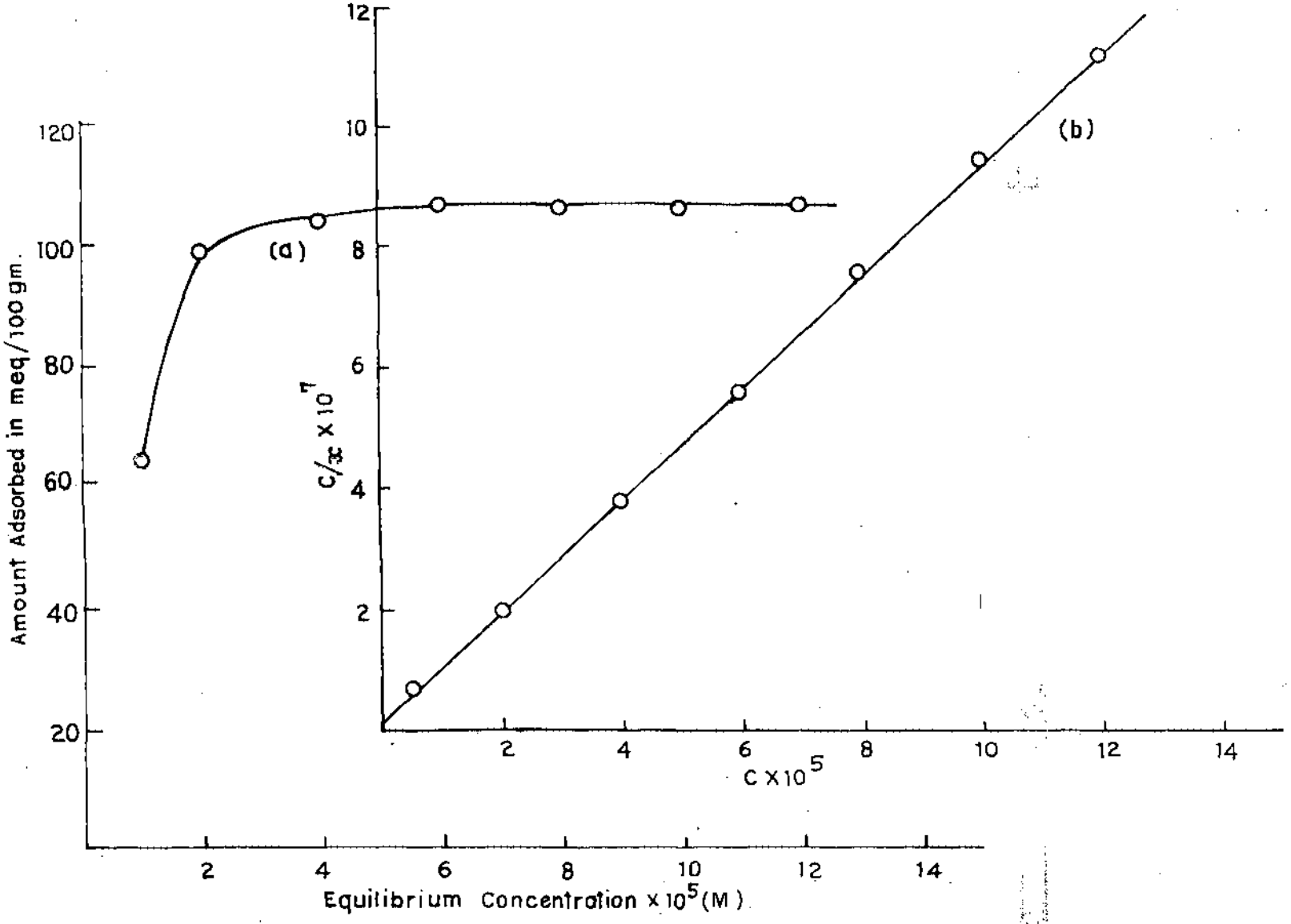

FIG. 78 ADSORPTION ISOTHERM AT 27°C (a) AND LANGMUIR PLOT (b) OF MMT (AZURE-C) ON Na-MONTMORILLONITE .

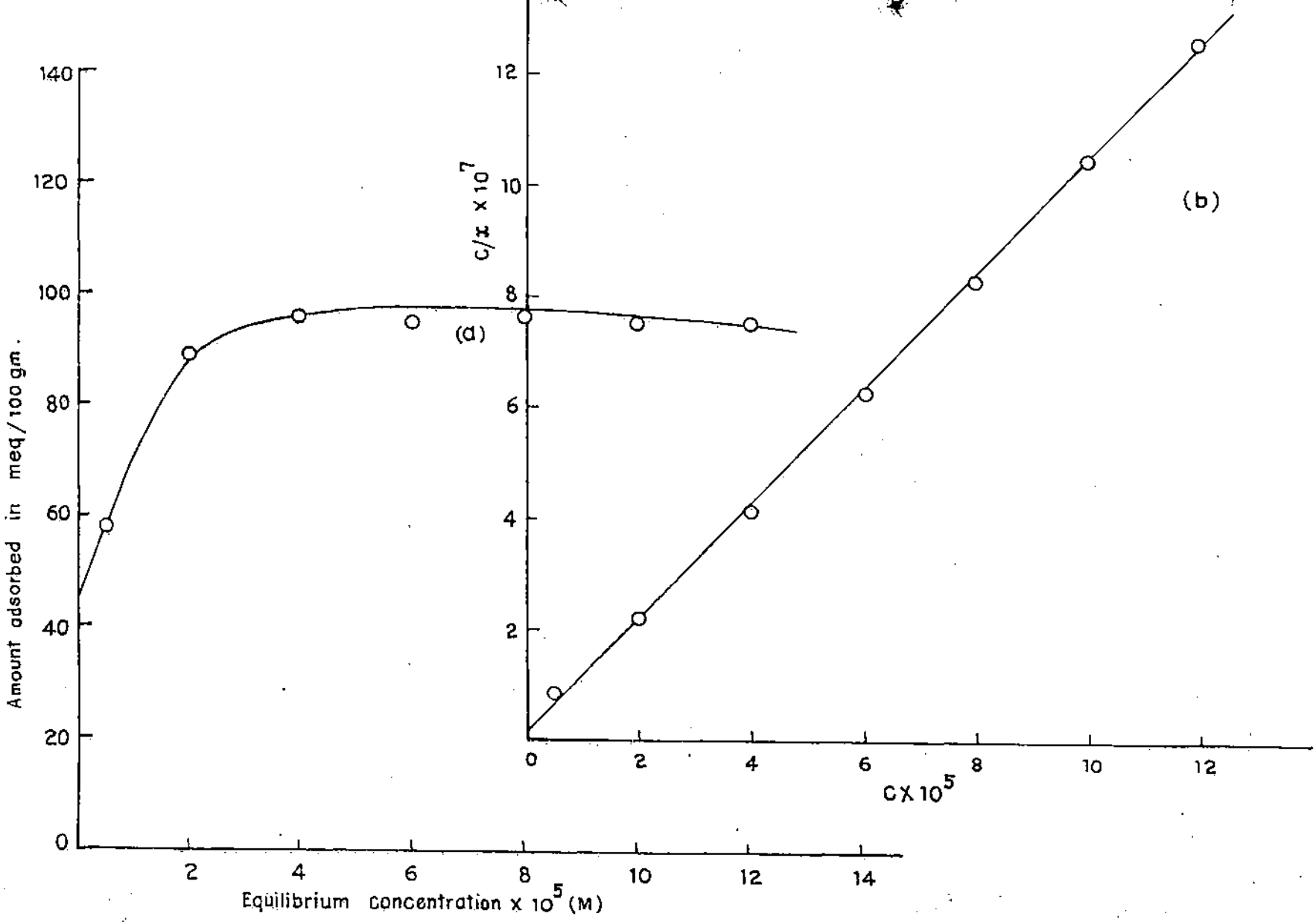

FIG. 79 ADSORPTION ISOTHERM AT 27°C (a) AND LANGMUIR PLOT (b) OF DMT (AZURE-A) ON Na-MONTMORILLONITE

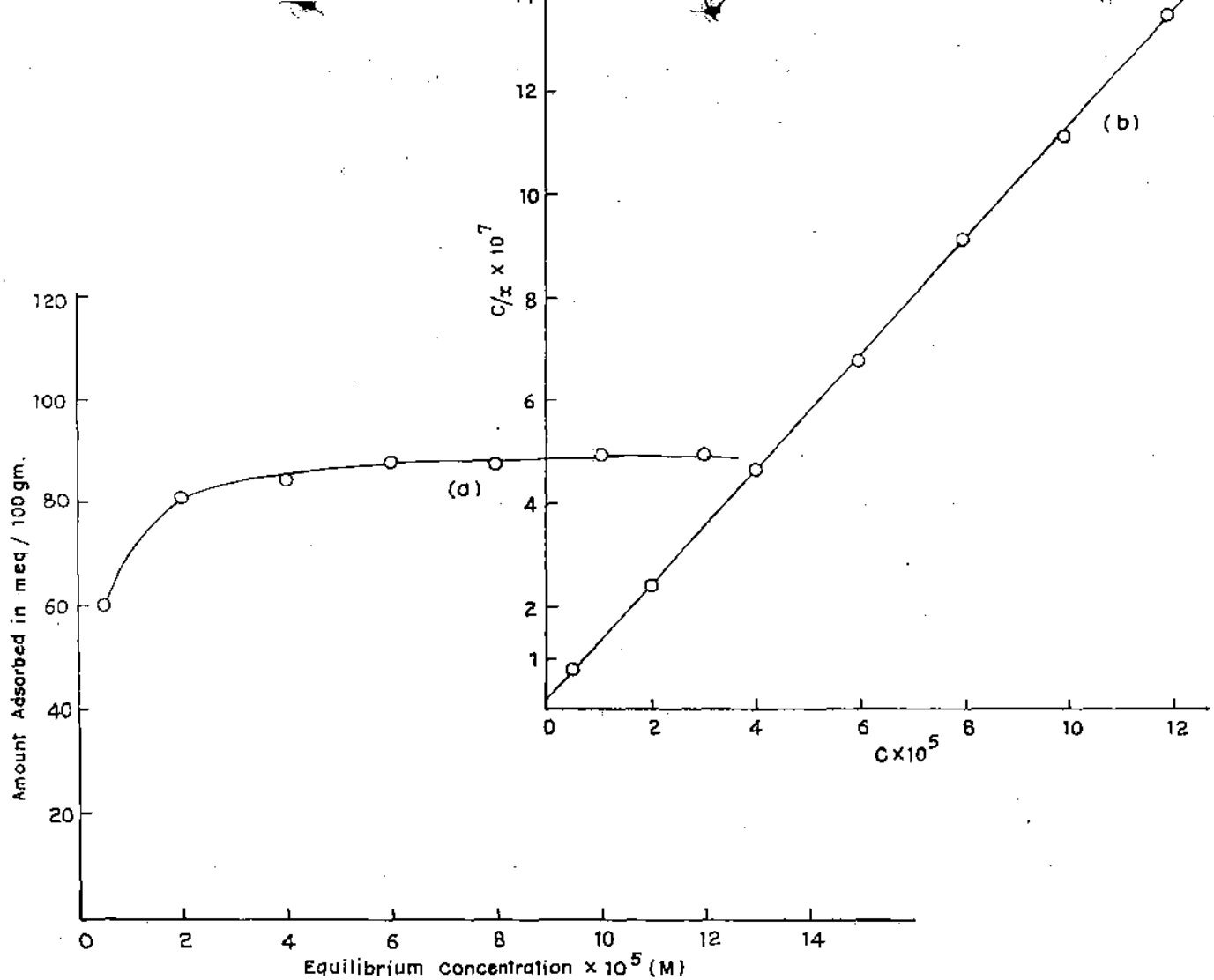

FIG. 80. ADSORPTION ISOTHERM AT 27°C (a) AND LANGMUIR PLOT (b) OF TMT (AZURE-B) ON Na-MONTMORILLONITE

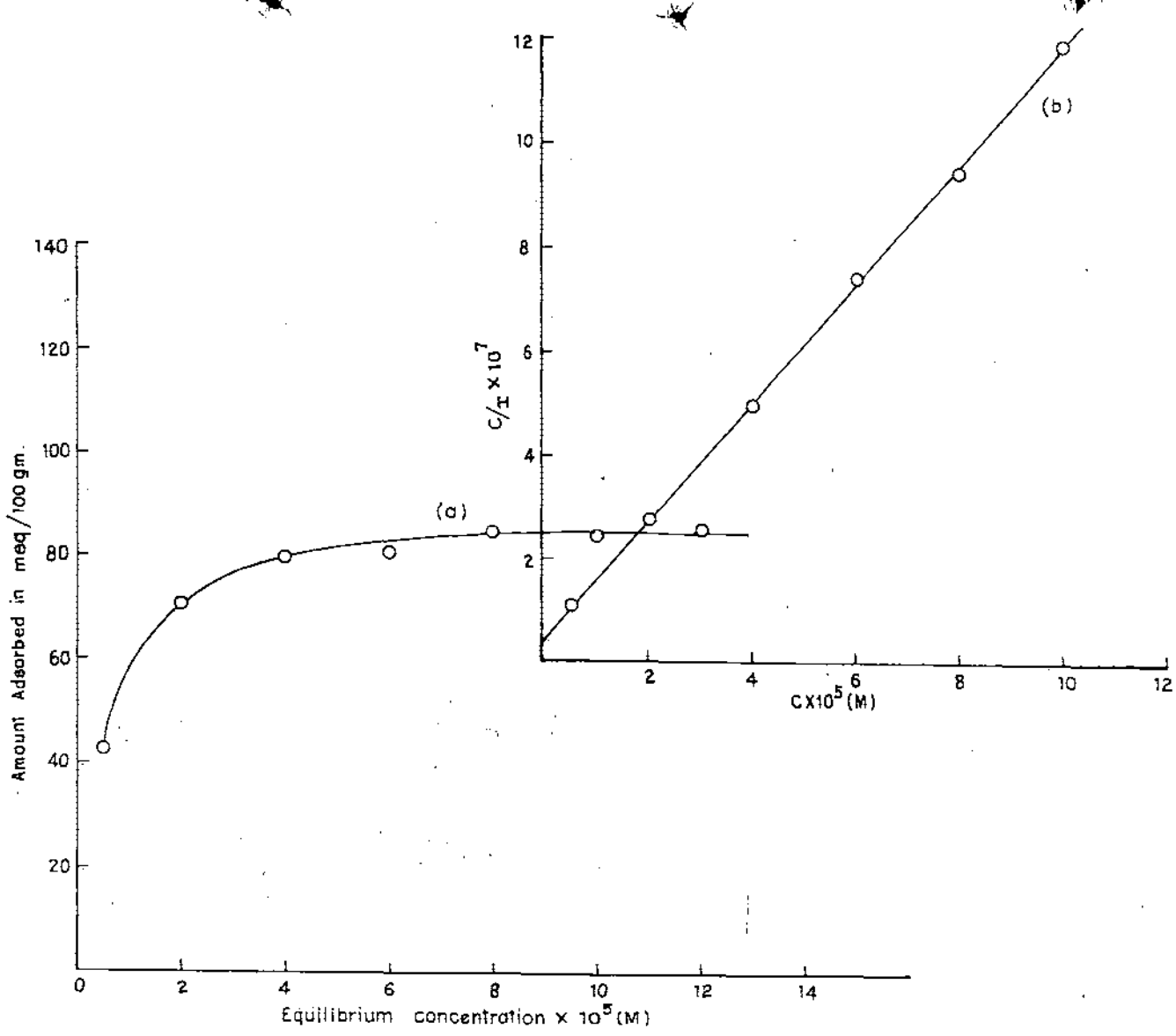

FIG. 81 ADSORPTION ISOTHERM AT 27°C (a) AND LANGMUIR PLOT (b) OF METHYLENE BLUE ON Na-MONTMORILLONITE

5.3.2 Studies on desorption

The desorption of the dyes from the clay complexes shows the extent to which the dyes are replaceable from the clay matrices and also the selectivities of different ions in the process. For the study of desorption process the experimental procedures have been described earlier (Section-5.2).

Desorption of Thionine:

The results of desorption of thionine from Na-montmorillonite-thionine complex by various inorganic and organic ions are presented in figs. 82-85.

Adsorption of thiazine dyes on montmorillonite is known to proceed through ion exchange process (153). So it is possible that descrption should also be an ion exchange process. Accordingly, an exchange equilibrium,

$$\bar{D}^{+} + \frac{i}{Z} i^{Z+} \rightleftharpoons \frac{\bar{i}}{Z} i^{Z+} + D^{+}$$

may be assumed where D stands for the dye, the bar denotes species in the clay phase and Z is the valency of the desorbing ion i. The selectivity coefficient is given by,

$$K_D^i = \frac{\left[\bar{i}^{Z+}\right]^{1/Z} \left[D^{+}\right]}{\left[\bar{D}^{+}\right] \left[i^{Z+}\right]^{1/Z}} \qquad \cdots\cdots\cdots\cdots (46)$$

where bracket means the concentration of the enclosed substances.

The concentrations used to calculate K_D^i are expressed in moles/dm^3 for the liquid phase. Since the values of the activity coefficient of thionine ions are not available in literature, the concentrations of the ions have been employed in the present work to calculate the selectivity coefficients and, therefore, the values are somewhat approximate.

The distribution coefficients have been calculated according to the equation

$$\lambda_i = \frac{\bar{m}_i}{m_i} \quad \ldots \quad \ldots \quad \ldots \quad \ldots \quad (47)$$

where $\bar{m}_i$ and m_i are the molal concentrations of the species i in the solid and liquid phases respectively.

The values of selectivity coefficients and distribution coefficients calculated by using the above relations for thionine are given in Table 23. The selectivity coefficient is a measure of the preference of the desorbing species i with respect to the dye for the mineral surface. If the value is less than 1.0, the species i has smaller affinity for the clay surface than the dye. If it is greater than 1.0, the adsorbent prefers species i to the dye ion and when it is equal to 1.0 which is very rarely observed, both the species will have equal affinities for the exchanger. It is, however, not a constant quantity and varies with the concentration of the species.

The values of the selectivity coefficients of the desorbing inorganic ions are less than 1.0 suggesting that the thionine ions are much preferred by montmorillonite to the monovalent, divalent and trivalent inorganic ions. By reason of their comparatively small sizes, these ions perhaps are unable to dislodge the sorbed dye ions from the clay matrix effectively. The selectivity coefficients of the inorganic ions may be placed in the order: $Na^+ < Li^+ < K^+ < NH_4^+ < Rb^+ < Cs^+$ for the monovalent cations, $Mg^{2+} < Ca^{2+} < Sr^{2+} < Ba^{2+}$ for the bivalent cations. The selectivity reversal of Li and Na, a deviation from the general lyotrope series, is to be noted. However, this type of behaviour has been observed by Gieseking and Jenny (143) on putnam clay (beidellite) and Das Kanungo and Chakravarti (301) in the desorption of Mg^{2+} ions from Mg-bentonite.

The distribution and selectivity coefficients of the monovalent organic ions are in the sequence: Cetyl pyridinium (CP) > Cetyltrimethyl ammonium (CTMA) for the long chain surface active agents and tetrapropyl ammonium (TPA) > tetraethyl ammonium (TEA) > tetramethyl ammonium (TMA) for the tetraalkyl ammonium halides. It is seen that the efficiency of large organic cations is much greater than that of the inorganic ions in desorbing thionine from its Na-montmorillonite complex. The preference of large organic ions to the dye cation by the clay surface being thus indicated.

The exchange isotherms of thionine from its Na-montmorillonite complex by tetraalkyl ammonium ions, the long chain cetyltrimethyl ammonium and pyridinium ion are presented in figs. 84-85. It is observed that the extent of desorption in each case increases with

chain length of the organic ions; this may be attributed to the increased contribution of vander Waals forces to the adsorption energy (146,300) as well as to the change in the hydration status of the ions in the clay interlayer. Such exchange behaviour would, however, be expected for a flat orientation of the ions at the clay surface as vander Waals type of interactions are additive and, therefore, would increase with the size of the interacting species. It is interesting to note that the extent of the dye released from the clay matrix is higher with comparatively smaller $(C_3H_7)_4N^+$ ions than with the larger CP^+ or $CTMA^+$. This may be explained from the covering-up effect of some of the exchange sites by the larger surface active ions lying flat onto the surface (233) and consequently a fraction of thionine initially adsorbed by the clay remaining unavailable for exchange. Further, among the surfactants the relative exchanging efficiency $CTMA^+ < CP^+$ may be related to their decreasing critical micelle concentration (cmc) values (302) which are 9.2×10^{-4}M and 9.0×10^{-4}M, respectively at 25°C.

It can be observed that although all the exchange isotherms are of the L-type, the desorption isotherms obtained with TEA^+, TPA^+, $CTMA^+$ and CP^+ are of "S" type in the classification of isotherms of Giles et al. (298). The C-type of curve was also observed by Greenland et al. (303) in the adsorption studies of aminoacids and peptides on Ca-montmorillonite and by Sarkar and Das Kanungo (304) in the desorption of tris-trimethylene diamine Co(III) ion, from its H-bentonite complex by 1,3 propane diammonium chloride. This type of curve represents constant partition between

the solution and surface, suggesting that new sites become available as solute is taken up by the microporous substrate and adsorption is always directly proportional to the solute concentration.

De et al. (299,305) earlier observed S-type of isotherms in the desorption of cationic dyes by $CTMA^+$ and CP^+ from clay-dye complexes. Usually the S-curve indicates co-operative adsorption, with solute molecules tending to be adsorbed or packed in rows or clusters. In the S-curve, the slope at first increases with concentration because sites capable of retaining a solute molecule increase in cooperative adsorption but eventually the slope falls and becomes nil at the saturation point when no vacant sites remain. This may explain the S-group of curves obtained in the desorption of thionine with TEA^+, TPA^+, $CTMA^+$ and CP^+. However, theoretical treatment for the classification of the solute adsorption isotherms by Giles et al. (306) shows that S-curve occurs when the activation energy for the desorption of the solute is concentration dependent, and/or is markedly reduced by large negative contribution of the solvent or a second solute. Greenland et al. (307) have illustrated the importance of the shape and size of the organic cations in determining the extent of vander Waals contact with the clay surface. The contribution of vander Waals force to adsorption energy would be greatest for those ions which are in closest contact with the surface, or enable close contact to be maintained with the adsorbed ions. Theng et al. (149) observed that tetra n-butyl and tetra n-propyl-ammonium ions were less strongly adsorbed in montmorillonite than might be expected from comparison with straight chain monoalkyl

ammonium ions of comparable number of carbon atoms, presumably due to the fact that the bulky but irregularly shaped tetrapropyl or tetrabutyl ammonium ions provide less intimate contact with the clay surface and hence the adsorption energy is less for them than for the latter ions. Therefore, for the straight chain larger organic ions like CP^+ or $CTMA^+$, the size is more important than charge in determining their preference for the aluminosilicate surface because the dispersion forces increase significantly with the length of the carbon chain. Moreover, the solubility of the organic cations in water decreases with the size of the ions, and so larger ions once adsorbed, have a lower tendency to return to the solution phase (308).

An attempt has been made to correlate the selectivity coefficient of the inorganic ions, which gives a relative measure of the affinities of the ions for the clay surface, with some other properties of the ions, viz. hydrated ionic radius (309) and the parameter, a^o, (310) of the Debye Huckel equation,

$$-\log \gamma_{\pm} = \frac{A Z_+ Z_- \sqrt{\mu}}{1 + B a^o \sqrt{\mu}} \quad \cdots \quad \cdots \quad \cdots \quad (48)$$

where the symbols have their usual significance. The selectivity coefficients have been plotted against hydrated ionic radii and the reciprocal of a^o i.e. the distance of closest approach of the two ions (Fig. 86). The latter plot has, however, been done on the basis of the simple electrostatic ion-exchange model of Pauley (311), which assumes that coulombic forces play the main role in the interaction between the counter ions and the charged clay surface

and that the counter ions in the ion exchanger are found at their distance of closest approach to the fixed ionic groups.

It may be noticed from the plot of log (selectivity coefficient) vs. hydrated ionic radius (309) of the monovalent ions (Fig. 86) that K^+, NH_4^+, Rb^+ and Cs^+ are more strongly attached to the clay surface than what should normally be expected of them from the values of their hydrated ionic radii. Thus, a distinct fixation tendency of these ions for the montmorillonite surface is indicated when compared with Li^+ and Na^+. The reason for such a selective sorption/fixation of these ions had earlier been thought as due to their close fit within the hexagonal cavities of basal oxygen planes (312-314) but the works of Shainberg and Kemper (224) and Kittrick (315) show that low hydration energy of the ions is the major factor in cation selectivity and fixation. Smaller the hydration energy, greater is the fixation tendency of the ion. Thus Cs^+ having the least hydration energy, is adsorbed the most. Further, cations with low hydration energy like K^+, NH_4^+, Rb^+, Cs^+ produce interlayer dehydration and layer collapse and are, therefore, fixed in interlayer position, while cations with high hydration energy such as Li^+, Na^+, Ca^{2+}, Mg^{2+}, Sr^{2+} and Ba^{2+} produce expanded interlayers and are not fixed (315). However, if log (selectivity coefficient) is plotted against $1/a^\circ$ of the alkali metal chlorides (310), a linear relationship is obtained as shown in fig. 86. With the alkaline earth chlorides both the hydrated ionic radius and $1/a^\circ$ yield straight lines with the selectivity coefficients. Fig. 86 clearly shows that in the displacement of thionine from its Na-montmorillonite complex by alkali metal chlorides, only $1/a^\circ$ may be used to correlate and

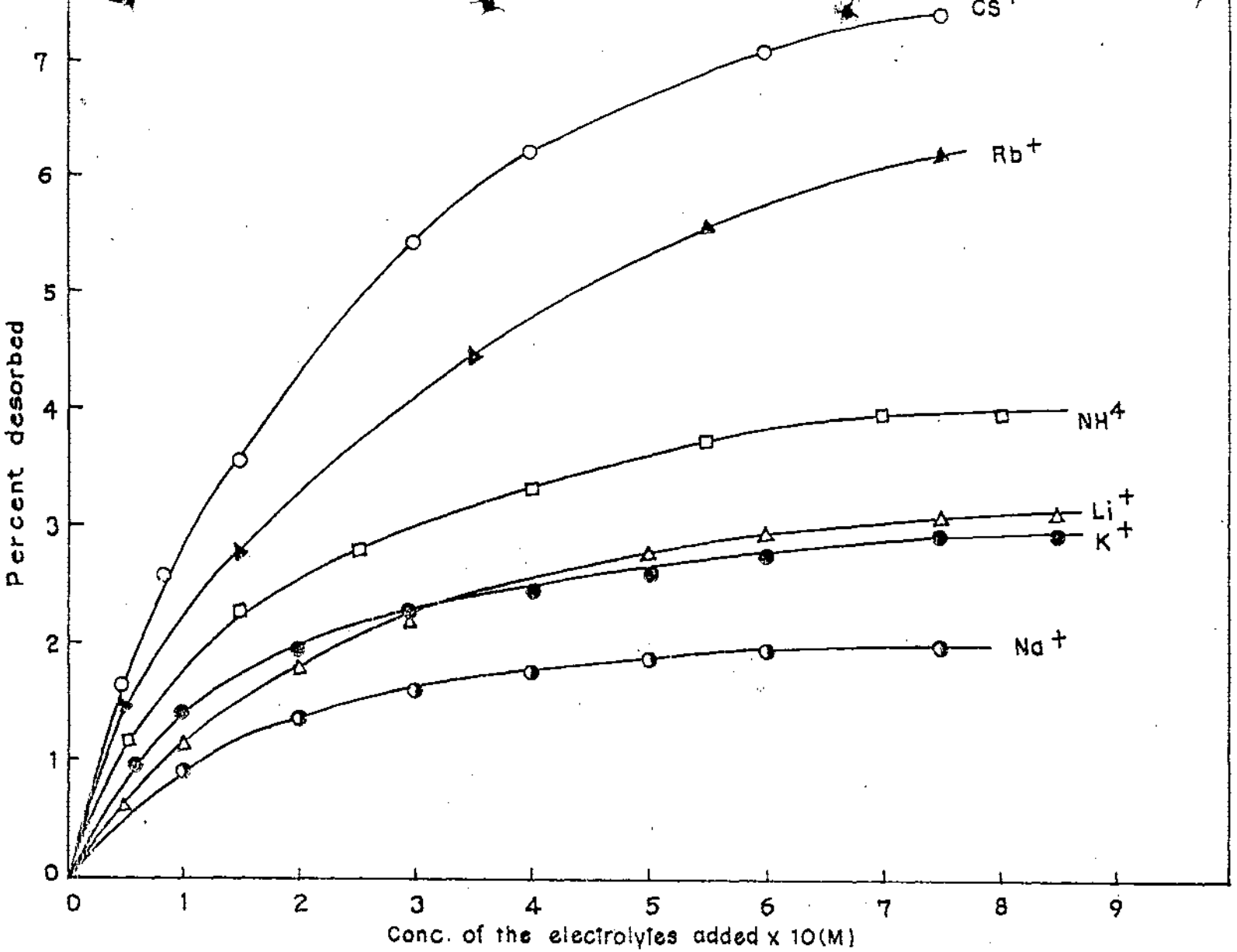

FIG. 82. DESORPTION OF THIONINE FROM Na-MONTMORILLONITE BY VARIOUS MONOVALENT IONS.

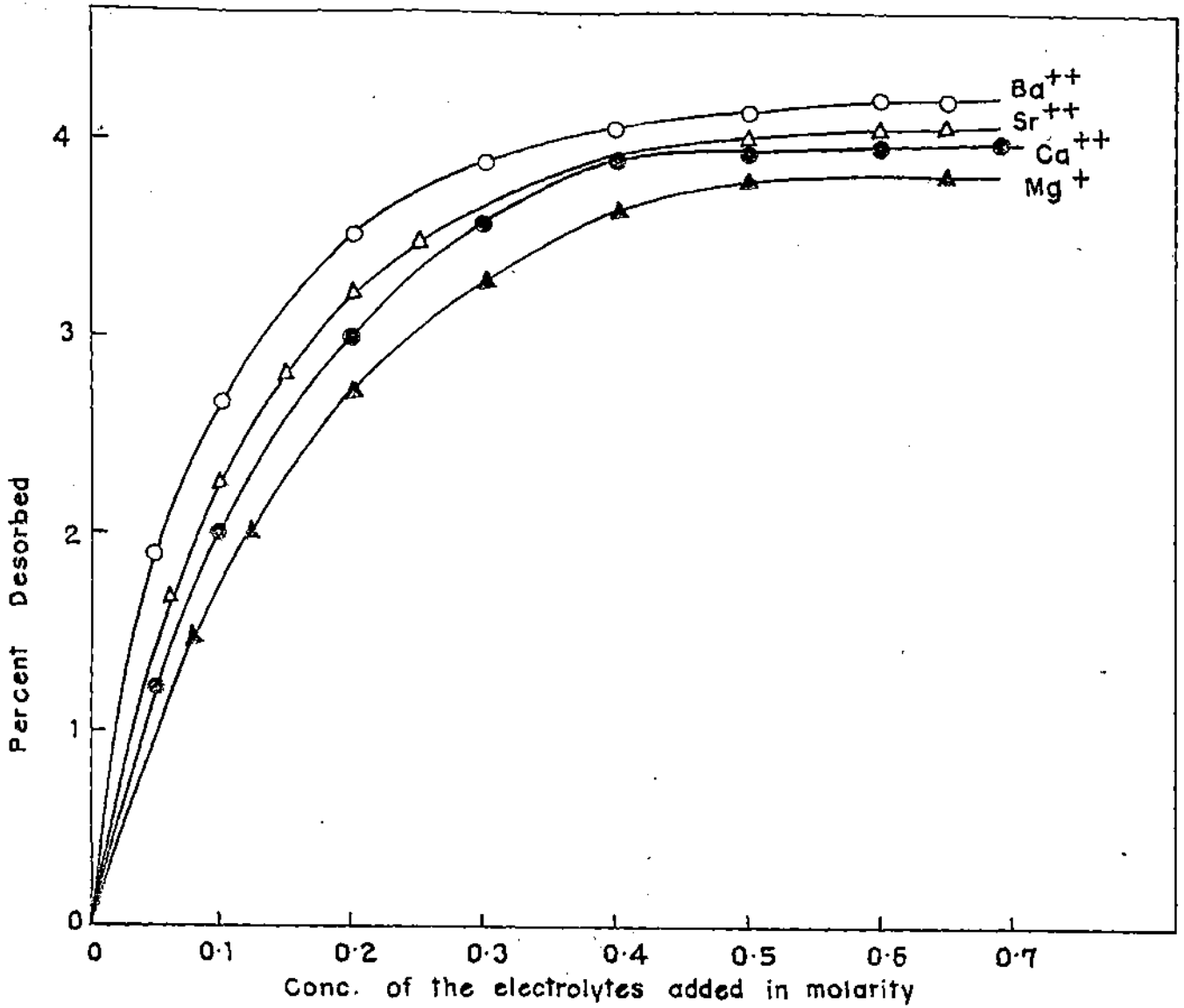

FIG. 83. DESORPTION OF THIONINE FROM Na-MONTMORILLONITE BY VARIOUS BIVALENT IONS.

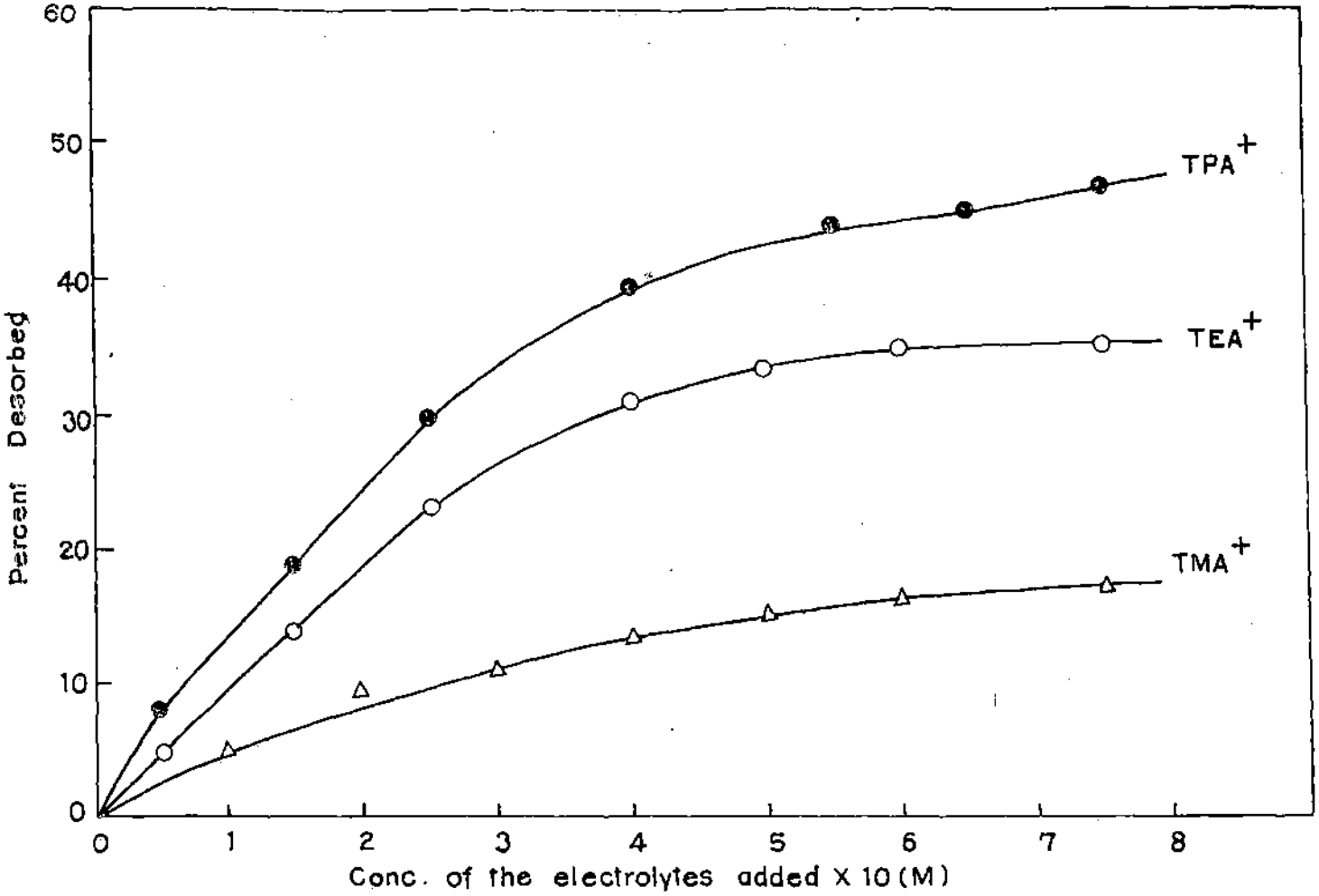

FIG. 84 . DESORPTION OF THIONINE FROM Na-MONTMORILLONITE BY VARIOUS TETRAALKYL AMMONIUM IONS .

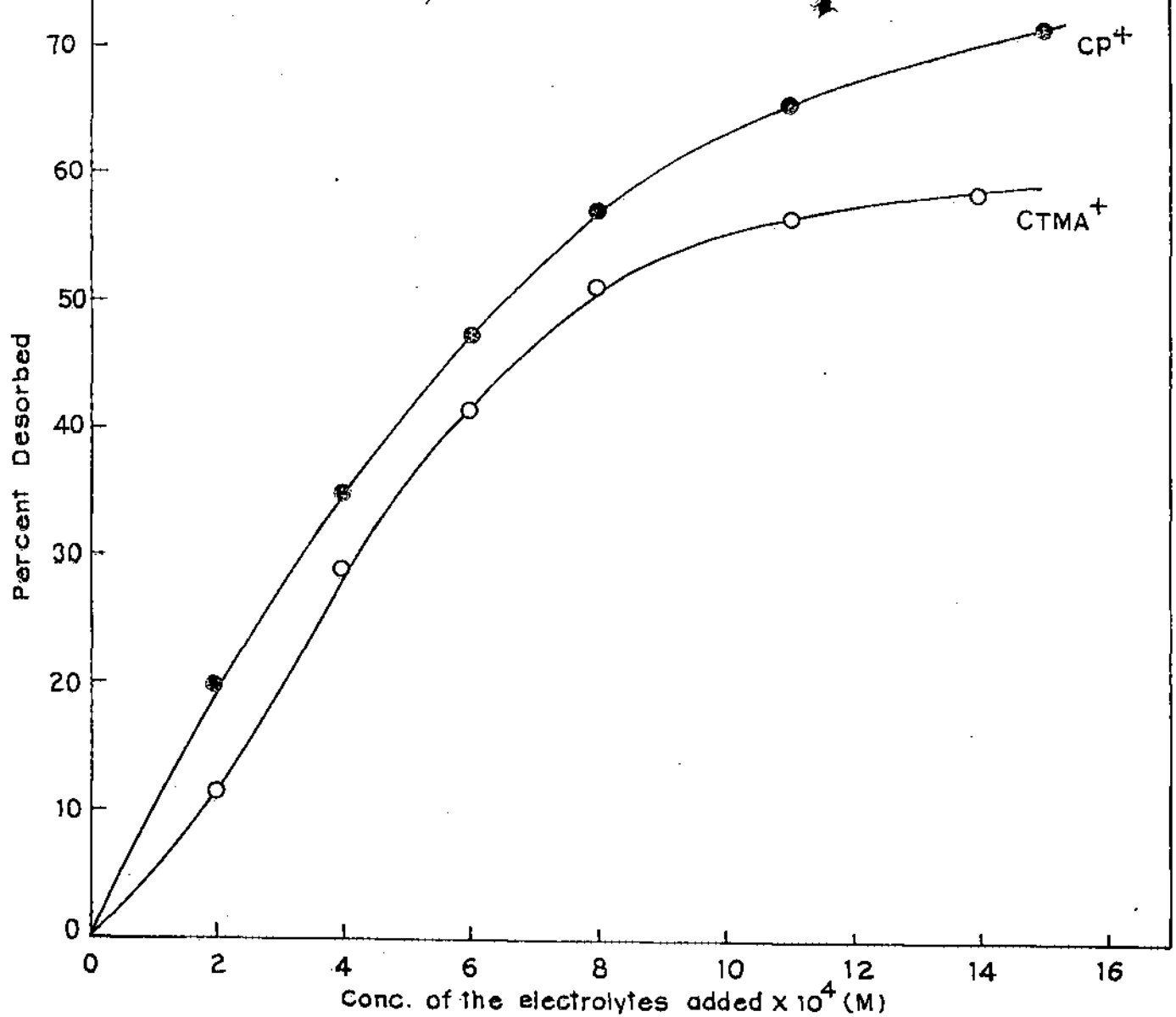

FIG. 85. DESORPTION OF THIONINE FROM Na-MONTMORILLONITE BY LONG CHAIN SURFACE ACTIVE TRIMETHYL AMMONIUM AND PYRIDINIUM IONS.

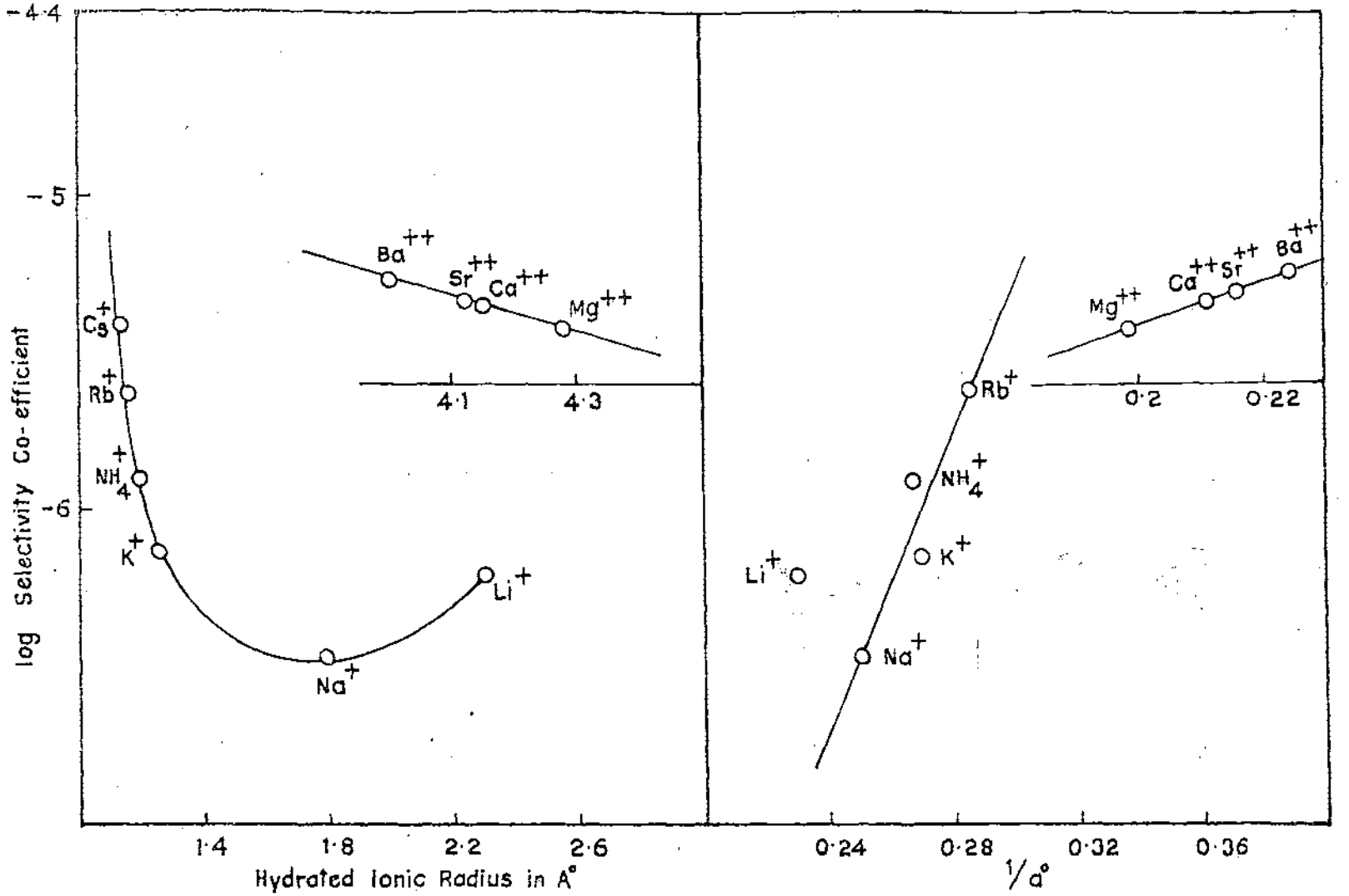

FIG. 86. CORRELATION OF SELECTIVITY COEFFICIENT WITH HYDRATED IONIC RADIUS AND DEBYE-HUCKEL PARAMETER a°, IN THE DESORPTION OF THIONINE FROM Na-MONTMORILLONITE-THIONINE.

predict the relative affinities of the ions for the mineral while for the alkaline earth metal chlorides both hydrated ionic radii and $1/a^{o}$ may be utilised for the purpose. The nonlinearity of the plot of log (selectivity coefficient) against hydrated ionic radius of the alkali cations may be attributed to the unequal fixation tendencies of these ions in the clay structure.

Thus, it appears that the plot of log (selectivity coefficient) vs. hydrated ionic radius may be used to detect ion fixation within the same valency type vis-a-vis layer collapse in ion exchangers especially in expanding type clay minerals. Furthermore, the obedience of the desorption data to the Pauley's model suggests that coulombic forces play the major roles in the interaction between the counter ions and the charged exchanger surfaces.

Desorption of azure C (MMT), azure A (DMT), azure B (TMT) and methylene blue.

The desorption isotherms of thionine derivatives from Na-montmorillonite complexes by inorganic and organic ions are shown in Figs. 87-102, and the calculated distribution and selectivity coefficients of the various electrolytes are recorded in tables 24-27.

The exchange isotherms with inorganic and organic desorbing ions are similar in nature to those obtained in the case of Na-montmorillonite-thionine complex but the extent of desorption with monovalent and bivalent inorganic ions is smaller for substituted thionines.

However, with the long chain surface active cetyl trimethyl ammonium ion and cetyl pyridinium ion the percentage of desorption is higher

presumably due to their bigger size.

According to their performance as desorbing agents, the ions are placed as,

a) $Na^+ \gtrsim Li^+ < K^+ < NH_4^+ < Rb^+ < Cs^+$

b) $Mg^{2+} < Ca^{+2} < Sr^{+2} < Ba^{+2}$

c) $TMA^+ < TEA^+ < TPA^+$

d) $CTMA^+ < CP^+$

The above desorption trend is almost similar for substituted thionines.(Fig. 87-102).

Compared to the inorganic ions, the percentages of exchange of the adsorbed dye with the organic ions are much higher and increases with the size of the ions. This is also reflected in the higher values of the distribution and selectivity coefficients (Table 24-27) of the latter ions. As in the case of thionine-montmorillonite, here also the desorption isotherms with TEA^+, TPA^+, TMA^+, $CTMA^+$ and CP^+ are S-shaped and may be explained in a similar manner (discussed earlier).

It is interesting to note that as high as 65% to 85% of the dyes can be displaced from the clay matrix by CP^+ and 60% to 70% of these dyes can be displaced from the clay matrix by $CTMA^+$. The desorption at the initial stage is perhaps the result of exchange of CP^+ and $CTMA^+$ in their monomeric forms with the clay bound dye but at higher concentration, it is effected by the micelles of these surfactants; CP^+ having lower CMC (9.0×10^{-4}M) than $CTMA^+$ (9.2×10^{-4}M) desorbs more. The initial steep portions of the exchange isotherms probably refer to the desorption of easily replaceable

dye ions and is followed by one having a much smaller slope, pointing to the existence of the more difficultly exchangeable dye cations.

The plot of log (selectivity coefficient) against $1/a^{o}$ of the alkali metal chlorides gives linear relationship while similar plot against hydrated ionic radius of the ions is not linear (Figs. 103-106). For the alkaline earth metal chlorides, however, both the parameters yield straight lines. An identical observation was made in Na-montmorillonite-thionine system and as such, similar conclusion may be drawn from the plots as in page 145 . It is observed from the desorption isotherms that the percentage of thionine desorbed as well as the calculated distribution and selectivity coefficients are always higher than those of substituted thionine. A close view on the values of distribution and the selectivity coefficients reveal that in general, the bonding strength of the dyes follow the order MB $\rangle$ TMT $\rangle$ DMT $\rangle$ MMT $\rangle$ Thionine. This is also reflected in the computed Langmuir bonding constants for the five adsorption isotherm which are 4.00×10^{5}, 5.0×10^{5}, 5.2×10^{5}, 5.75×10^{5} and $5.875 \times 10^{5} M^{-1}$ for thionine, MMT, DMT, TMT and methylene blue respectively. The higher value of the constant is suggestive of a stronger bonding of MB in Na-montmorillonite as the Langmuir bonding constant is directly proportional to the heat of adsorption (316). This observation is expected in view of greater size and lower solubility of substituted dyes as compared to thionine since vander Waals force increases significantly with the size of the organic ions. However, long chain surface active agents viz. $CTMA^{+}$ and CP^{+} showed some anomalous behaviour.

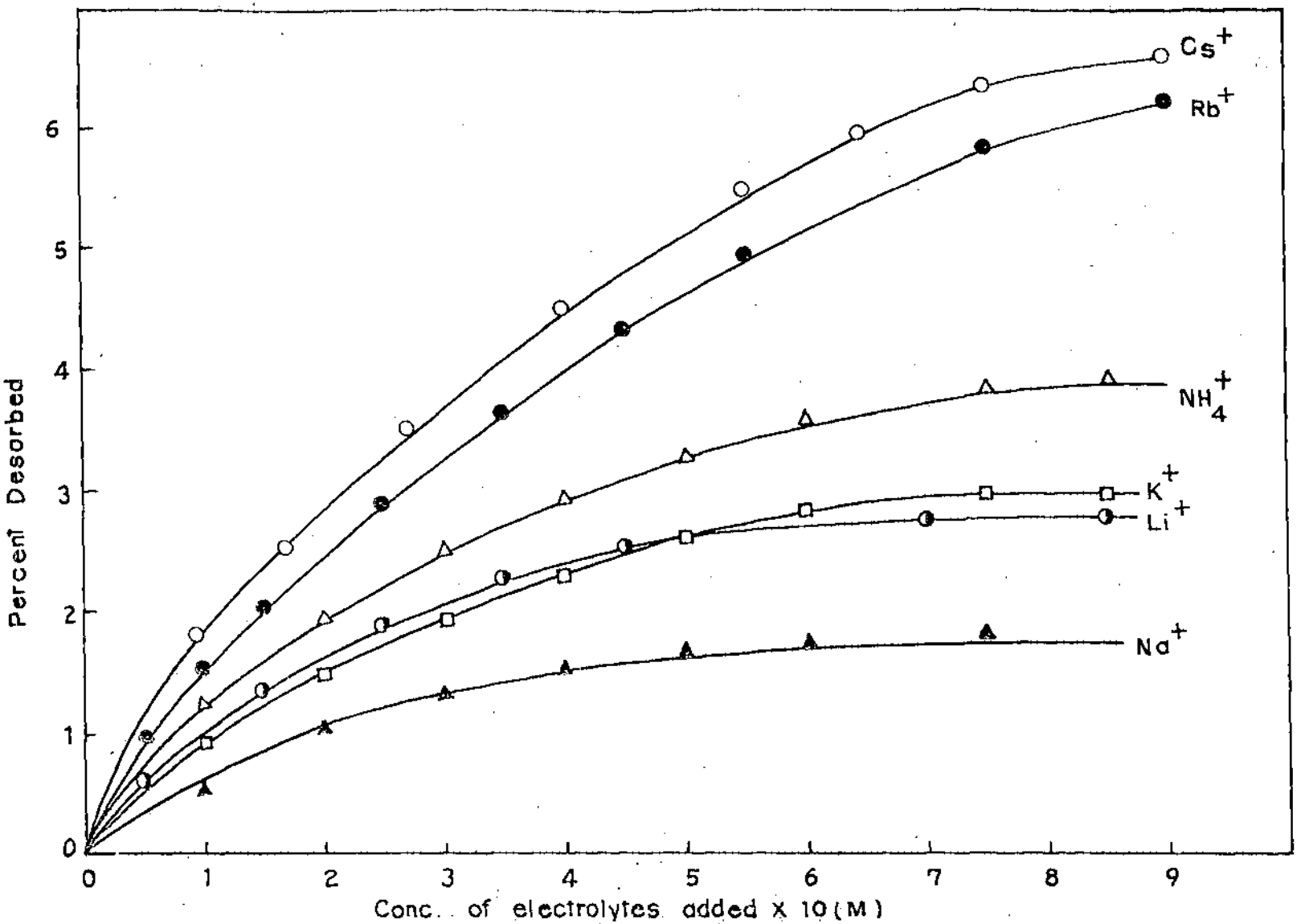

FIG. 87 DESORPTION OF MMT (AZURE-C) FROM Na-MONTMORILLONITE BY VARIOUS MONOVALENT IONS.

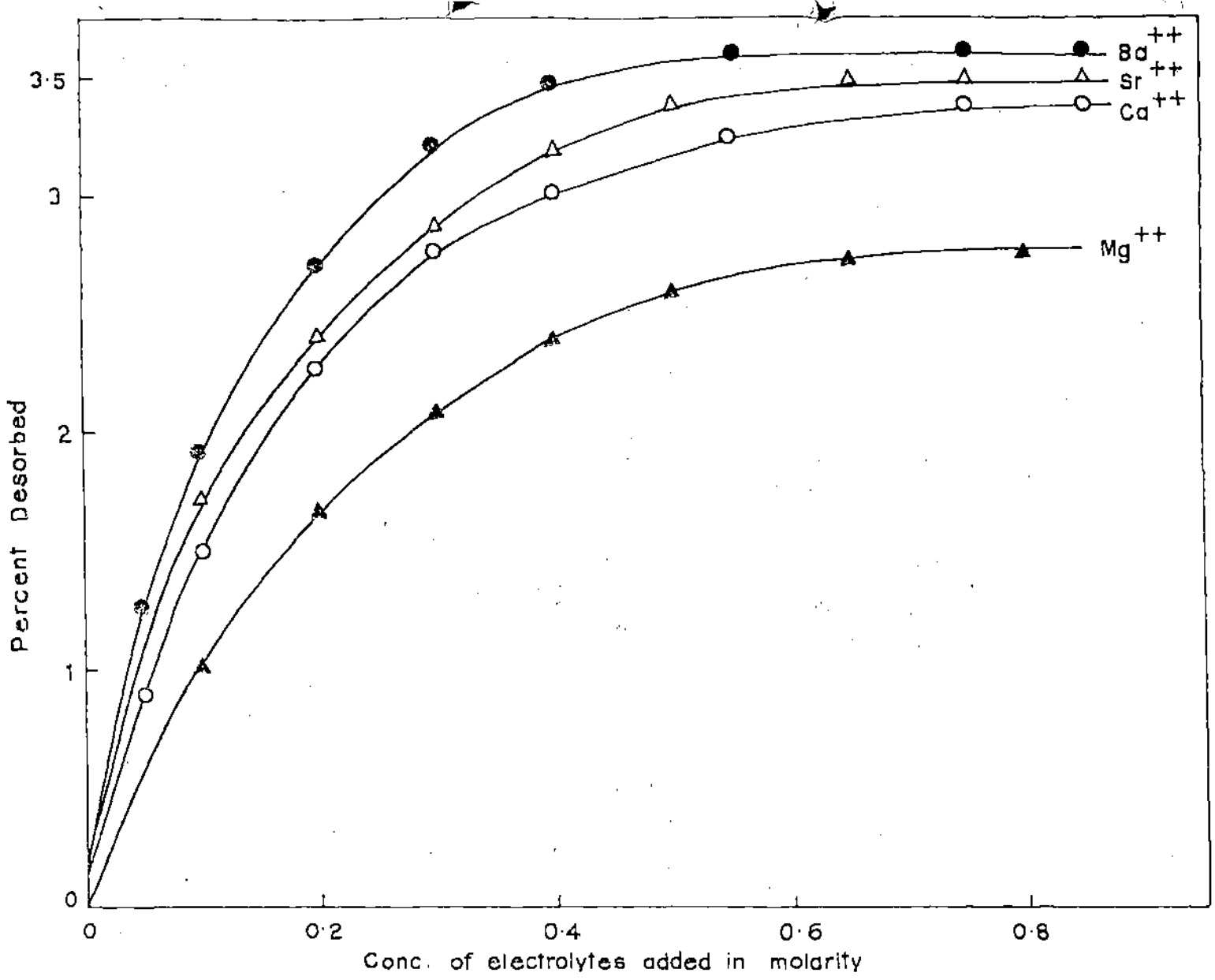

FIG. 88 DESORPTION OF MMT (AZURE-C) FROM Na-MONTMORILLONITE BY VARIOUS DIVALENT IONS.

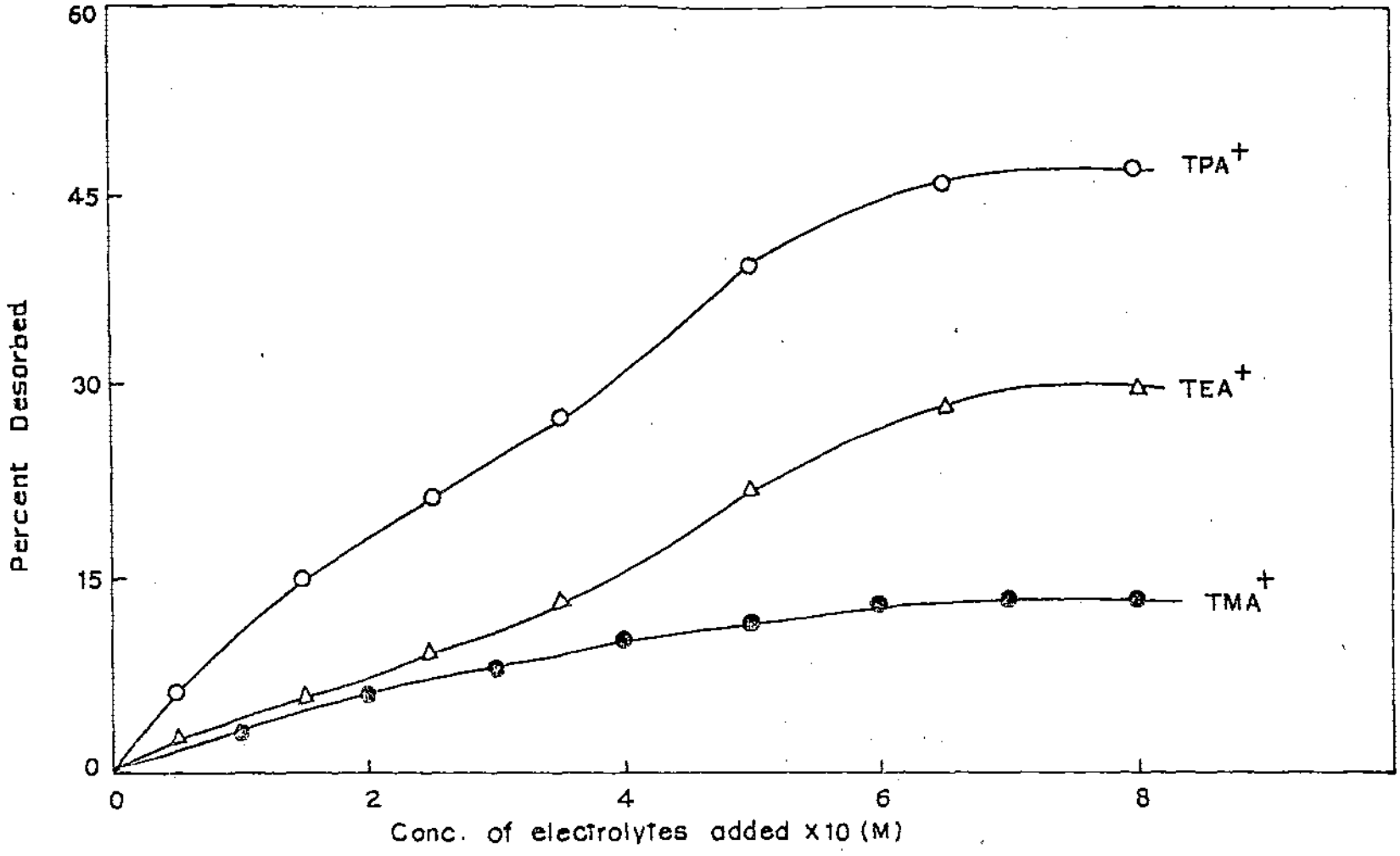

FIG. 89. DESORPTION OF MMT (AZURE-C) FROM Na- MONTMORILLONITE BY VARIOUS TETRA-ALKYL AMMONIUM IONS.

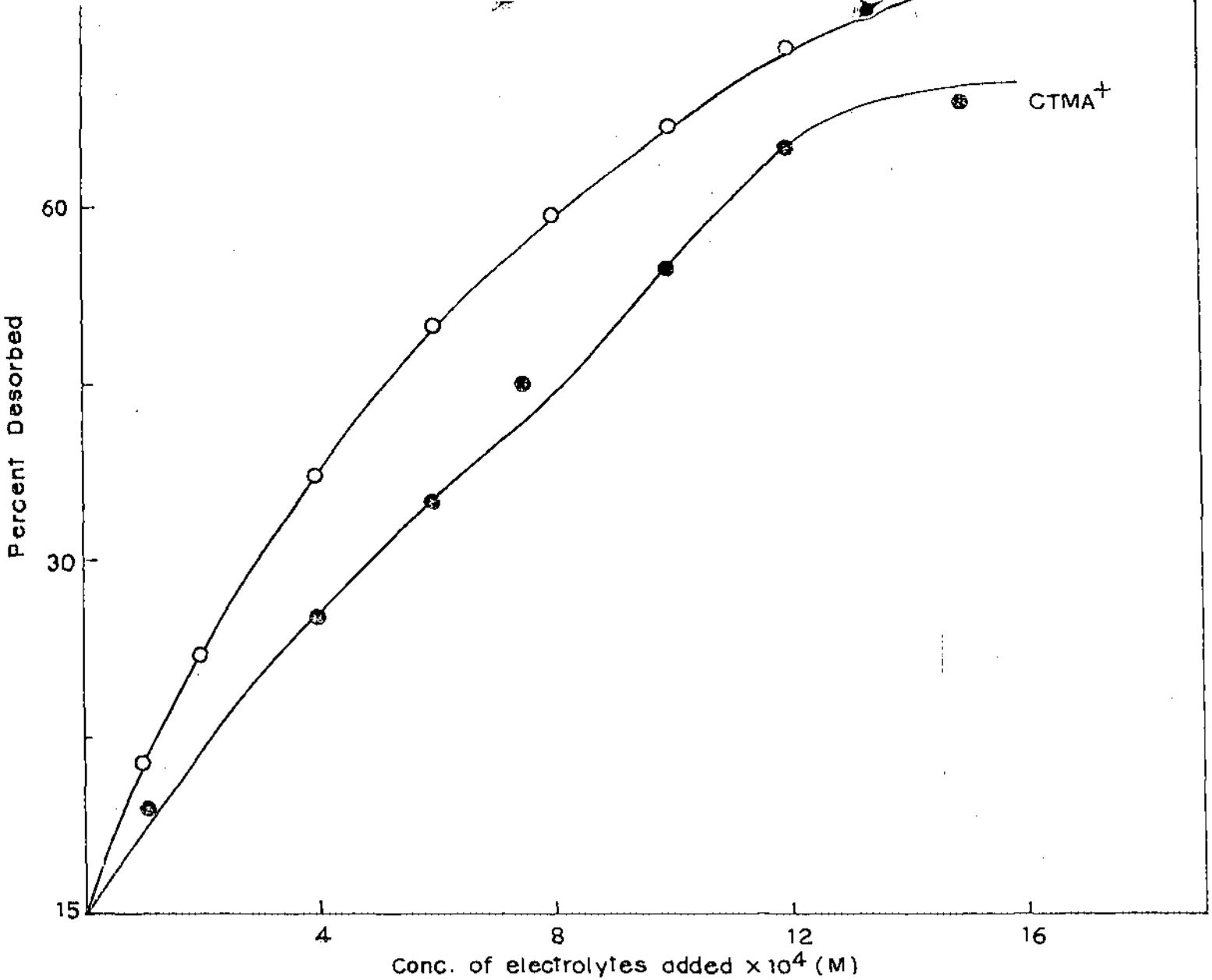

FIG. 90 DESORPTION OF MMT (AZURE-C) FROM Na-MONTMORILLONITE BY LONG CHAIN SURFACE ACTIVE TRIMETHYL AMMONIUM AND PYRIDINIUM IONS.

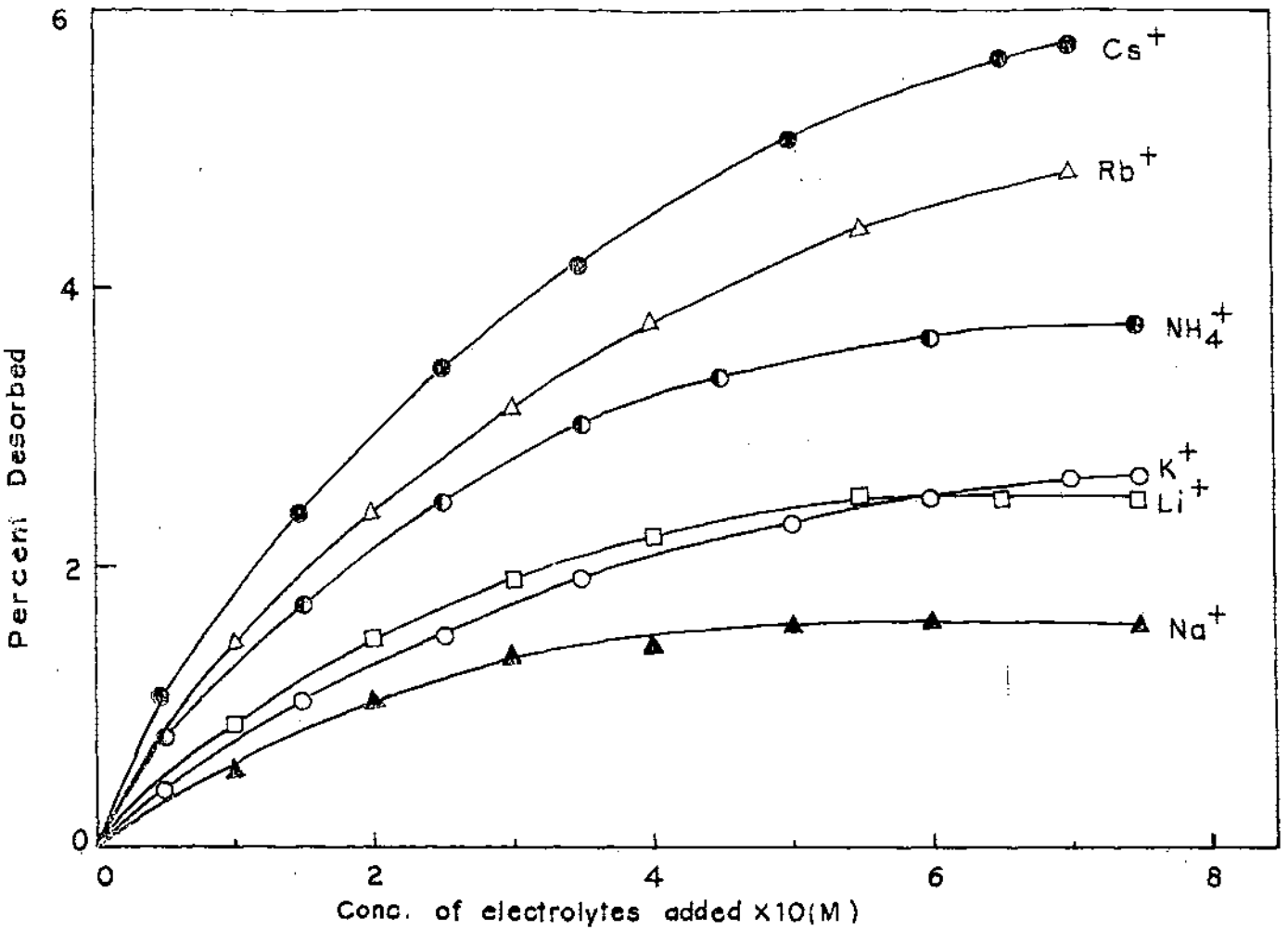

FIG. 91 . DESORPTION OF DMT (AZURE-A) FROM Na-MONTMORILLONITE BY VARIOUS MONOVALENT IONS.

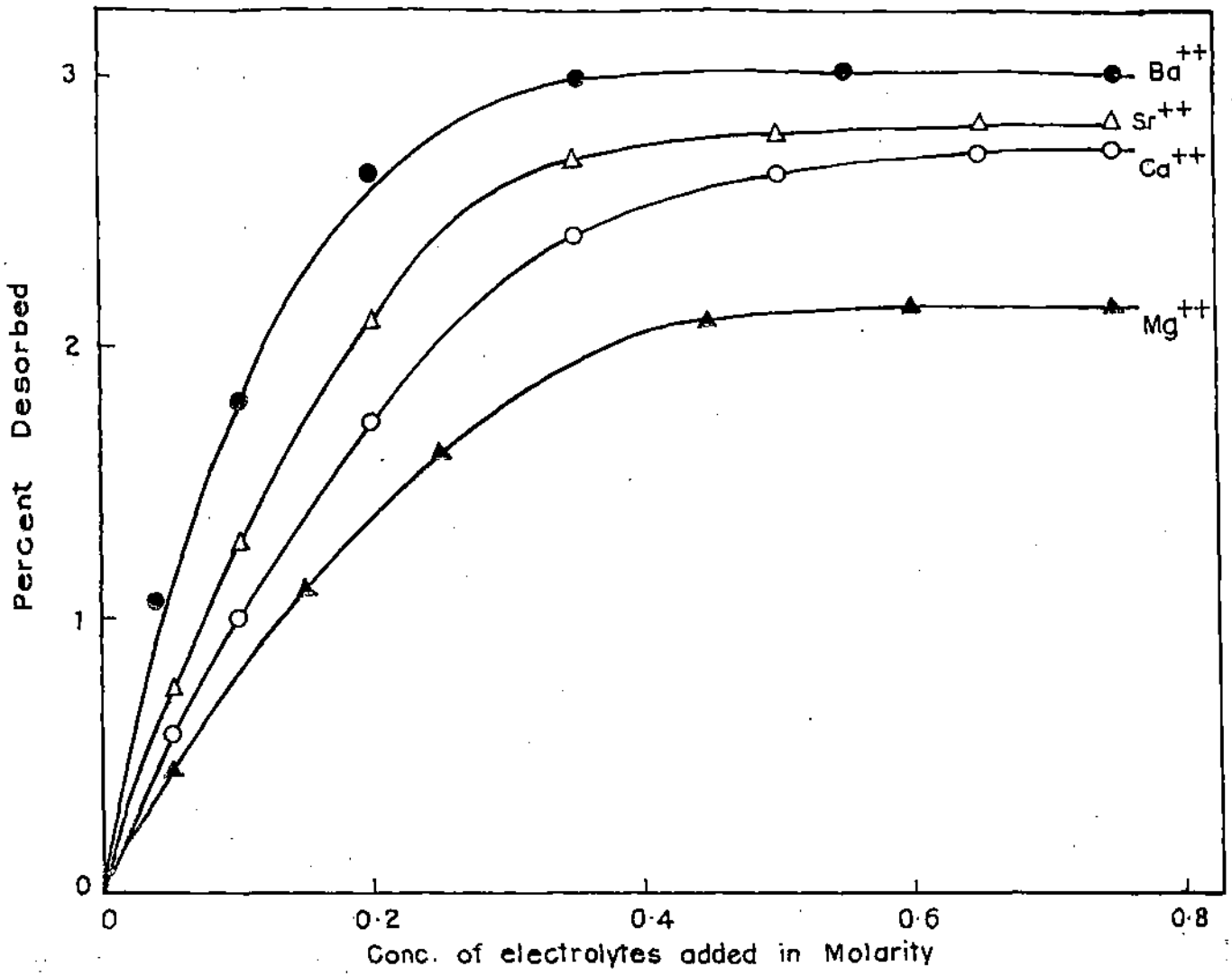

FIG. 92. DESORPTION OF DMT (AZURE-A) FROM Na- MONTMORILLONITE BY VARIOUS DIVALENT IONS.

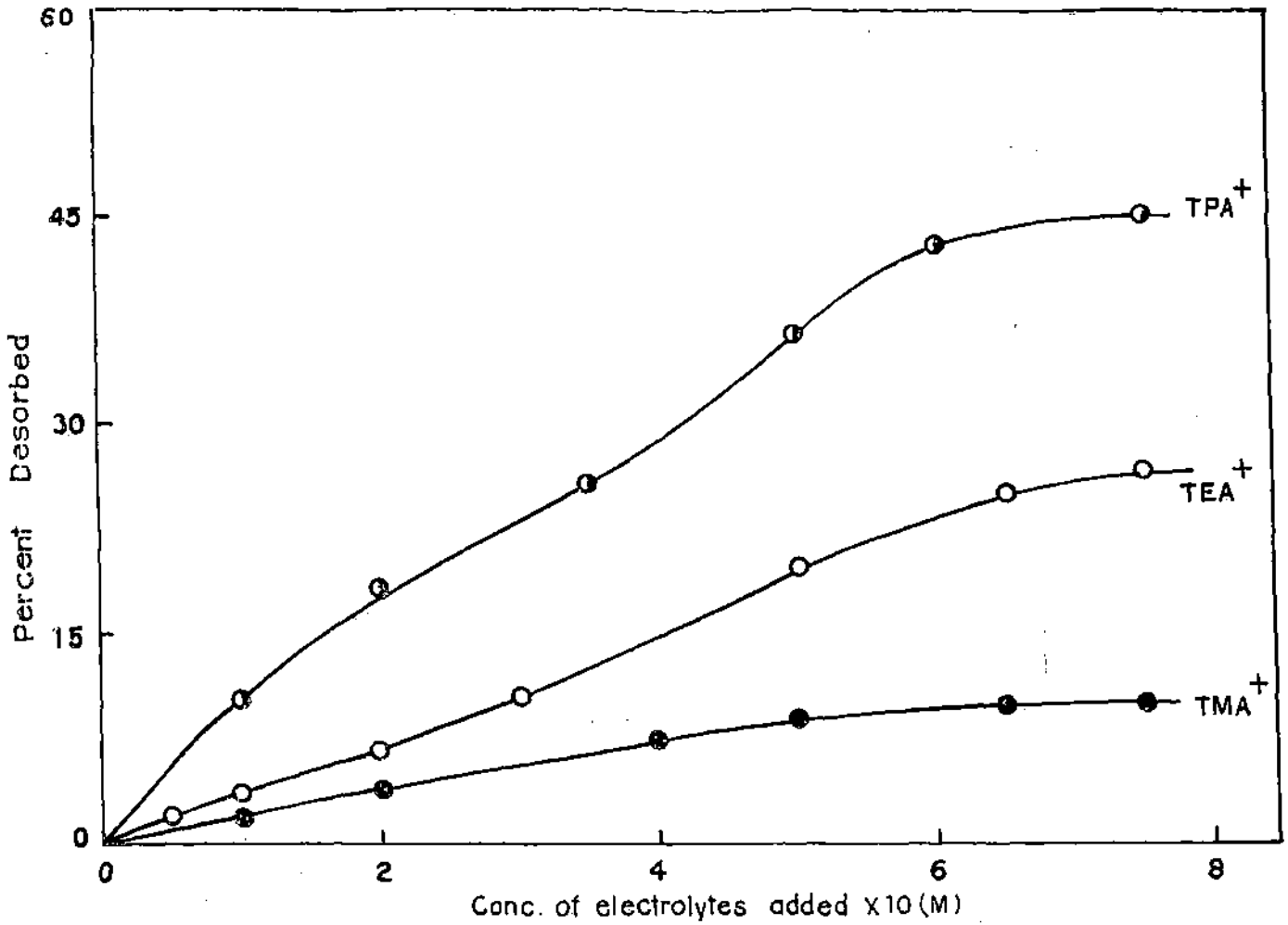

FIG. 93. DESORPTION OF DMT (AZURE-A) FROM Na-MONTMORILLONITE BY VARIOUS TETRA-ALKYL AMMONIUM IONS.

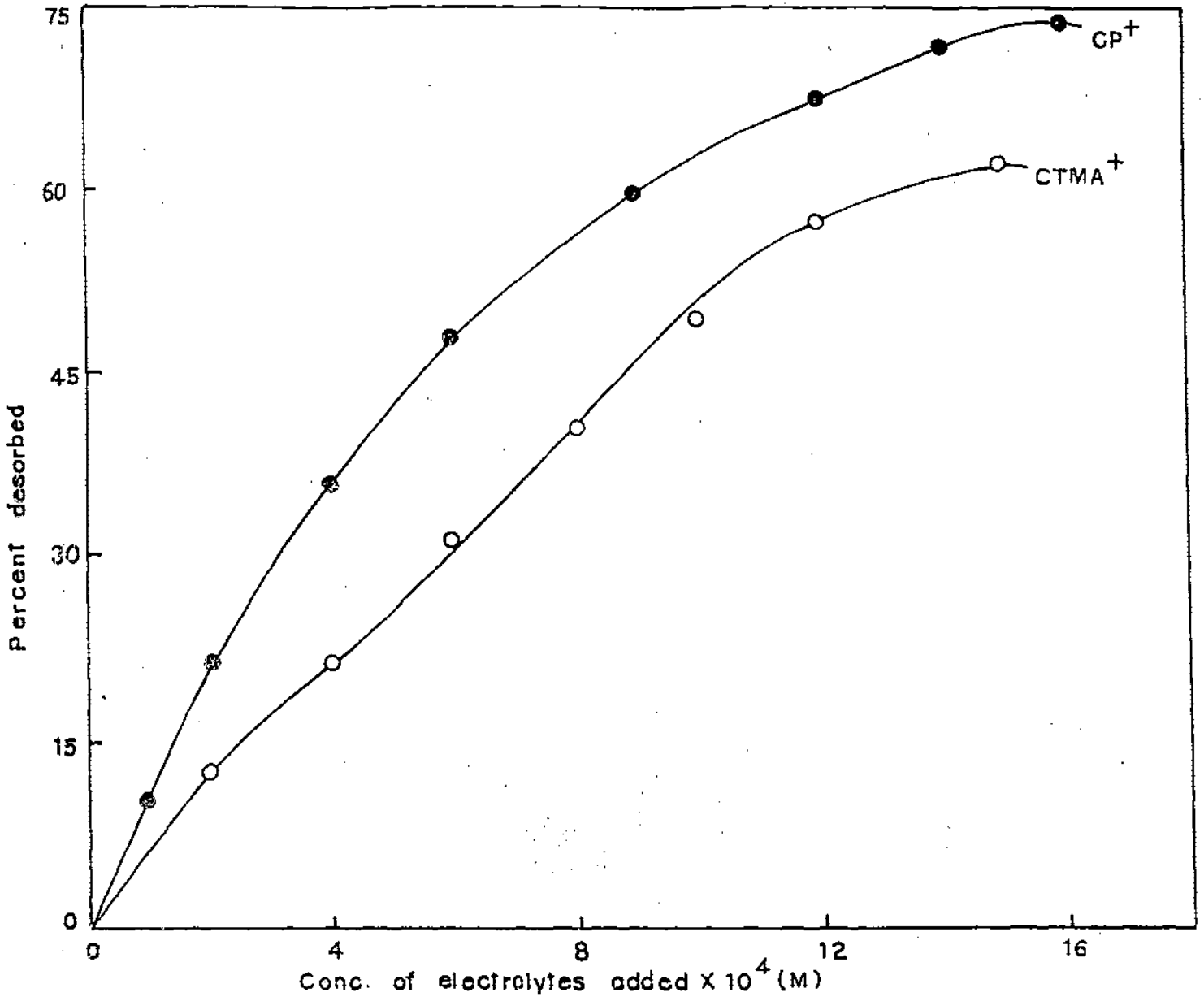

FIG. 94. DESORPTION OF DMT (AZURE-A) FROM Na-MONTMORILLONITE BY LONG CHAIN SURFACE ACTIVE TRIMETHYL AMMONIUM AND PYRIDINIUM IONS.

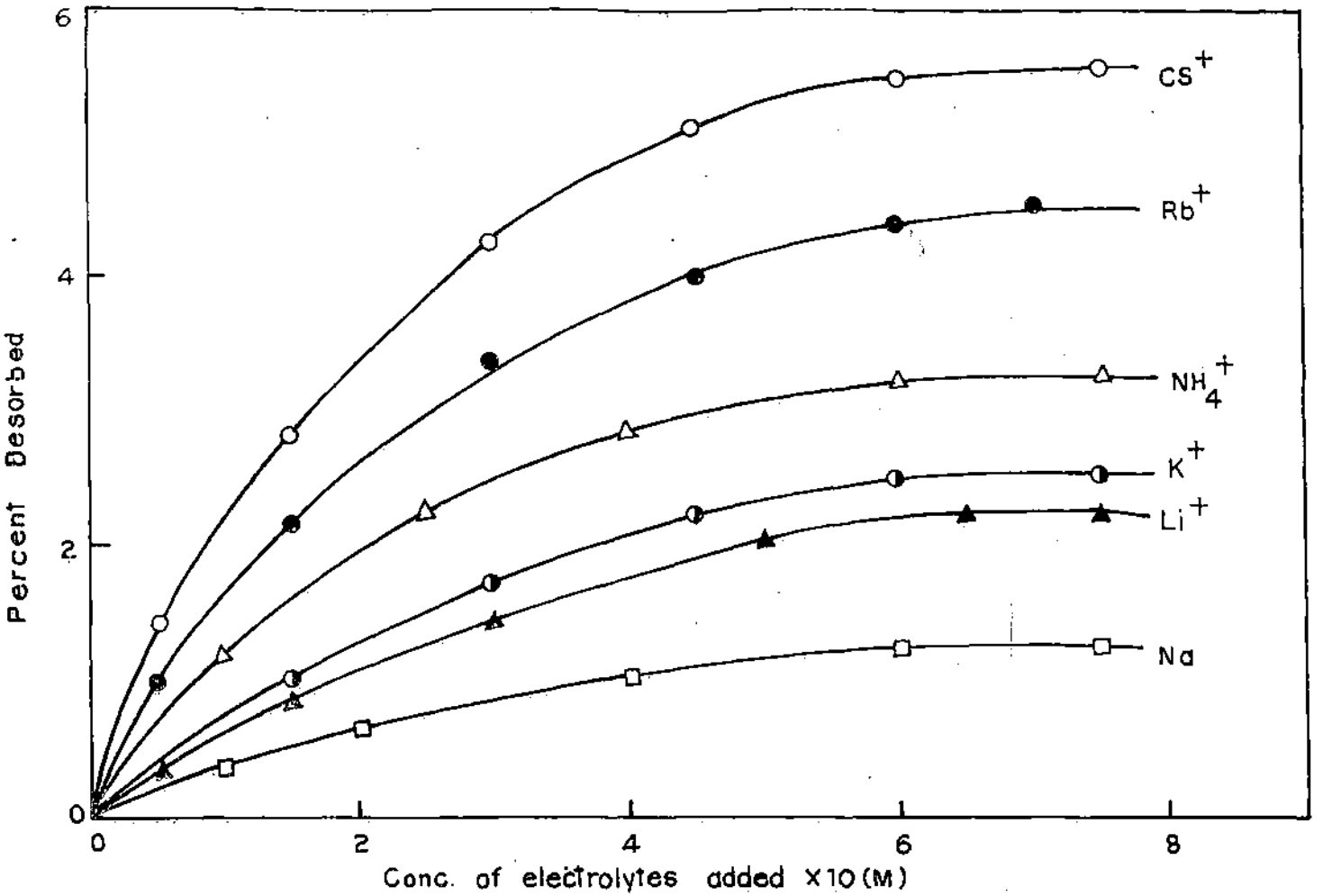

FIG. 95 DESORPTION OF TMT (AZURE-B) FROM Na-MONTMORILLONITE BY VARIOUS MONOVALENT IONS.

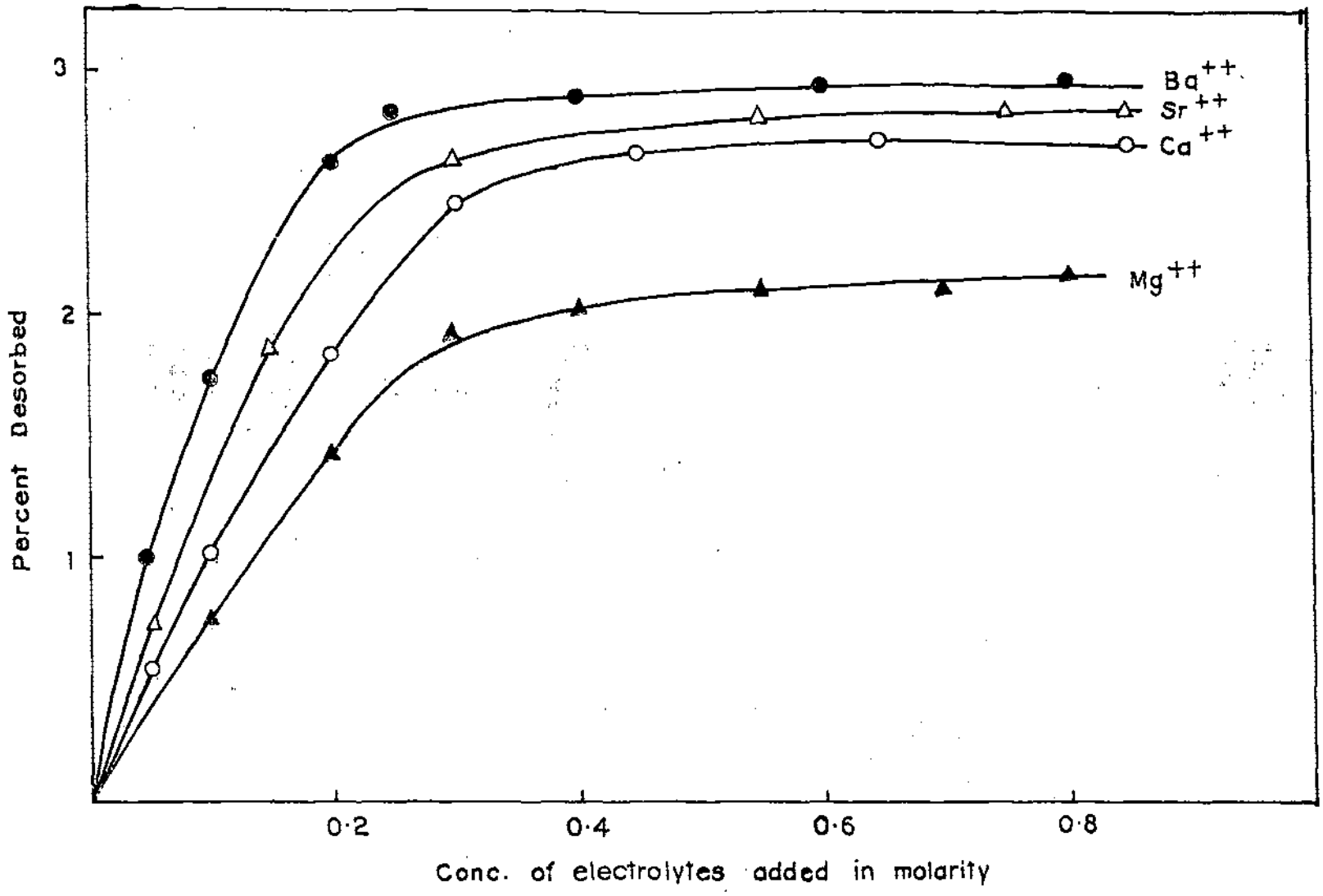

FIG: 96 DESORPTION OF TMT (AZURE-B) FROM Na-MONTMORILLONITE BY VARIOUS DIVALENT IONS.

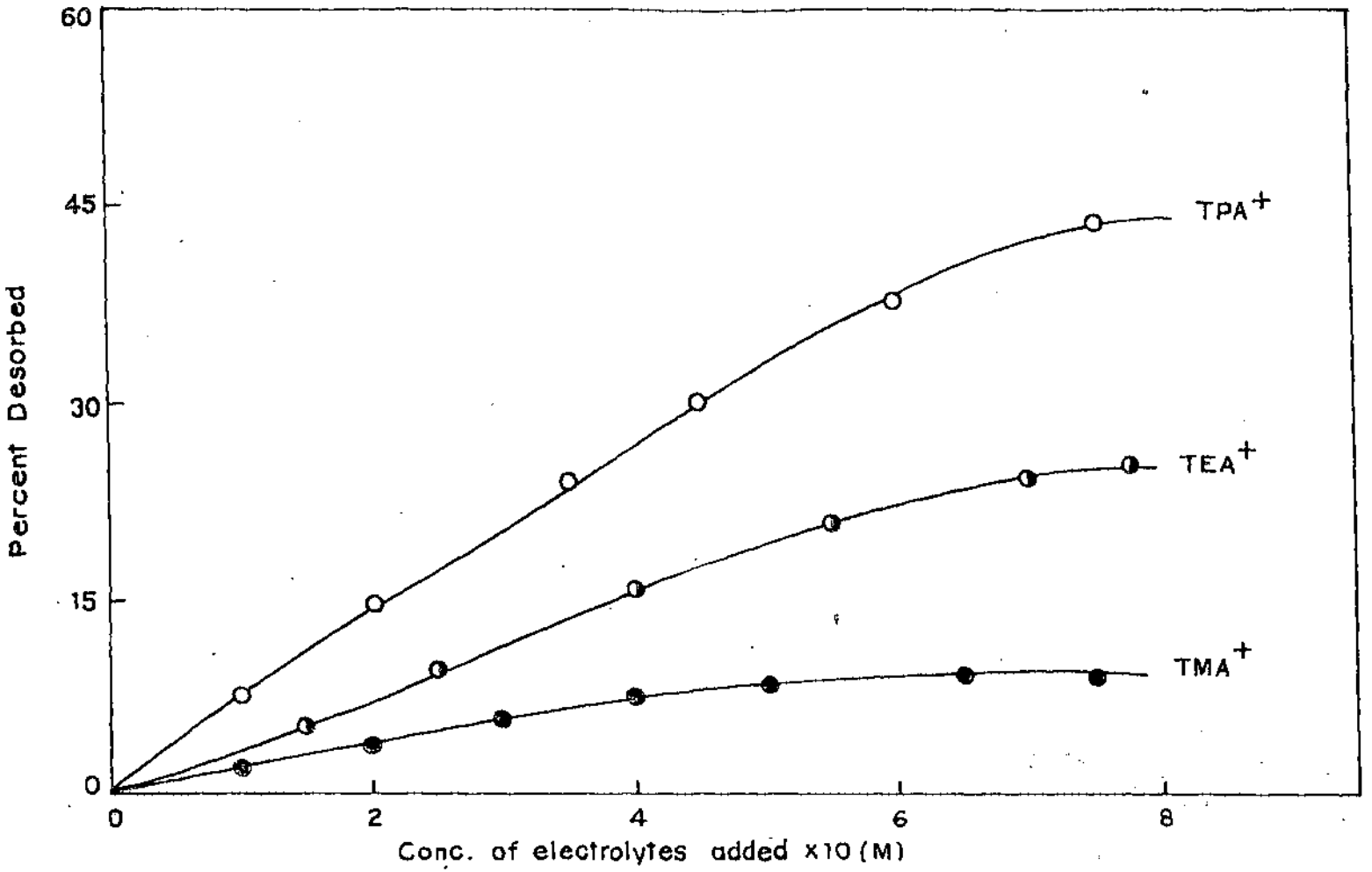

FIG. 97. DESORPTION OF TMT(AZURE-B) FROM Na- MONTMORILLONITE BY VARIOUS TETRA-ALKYL AMMONIUM IONS.

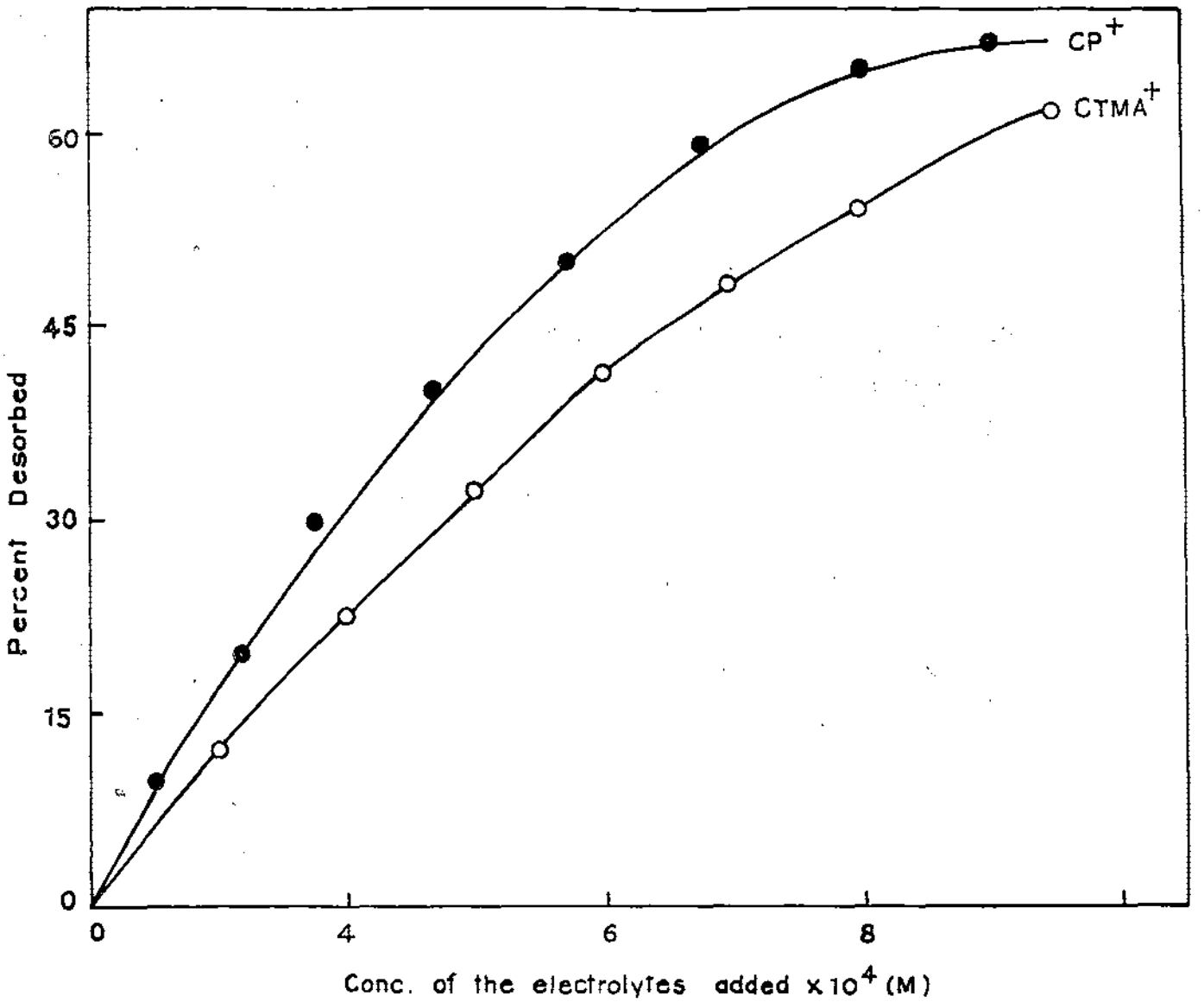

FIG. 98 DESORPTION OF TMT (AZURE-B) FROM Na-MONTMORILLONITE BY LONG CHAIN SURFACE ACTIVE TRIMETHYL AMMONIUM AND PYRIDINIUM IONS.

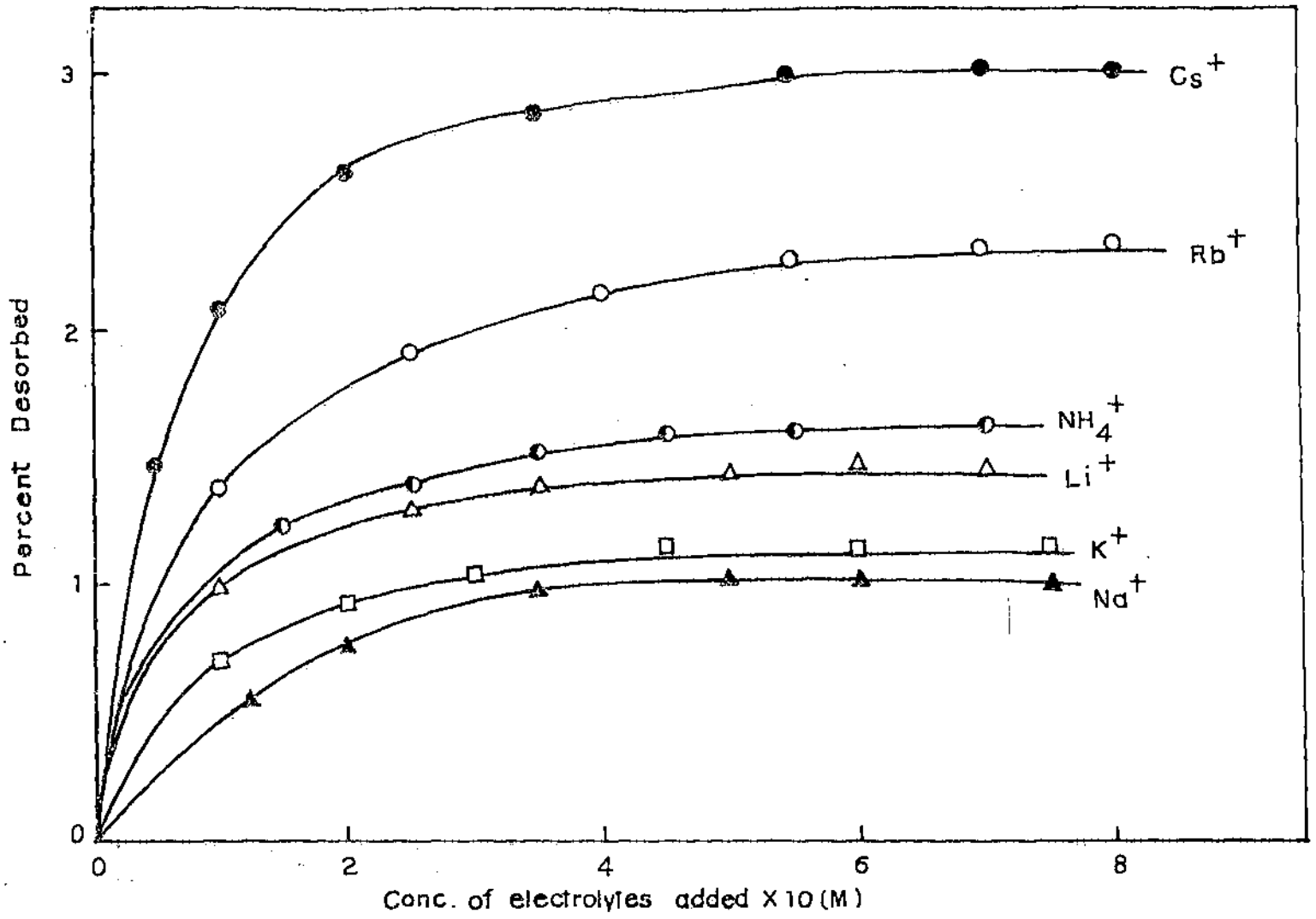

FIG. 99. DESORPTION OF METHYLENE BLUE FROM Na- MONTMORILLONITE BY VARIOUS MONOVALENT IONS.

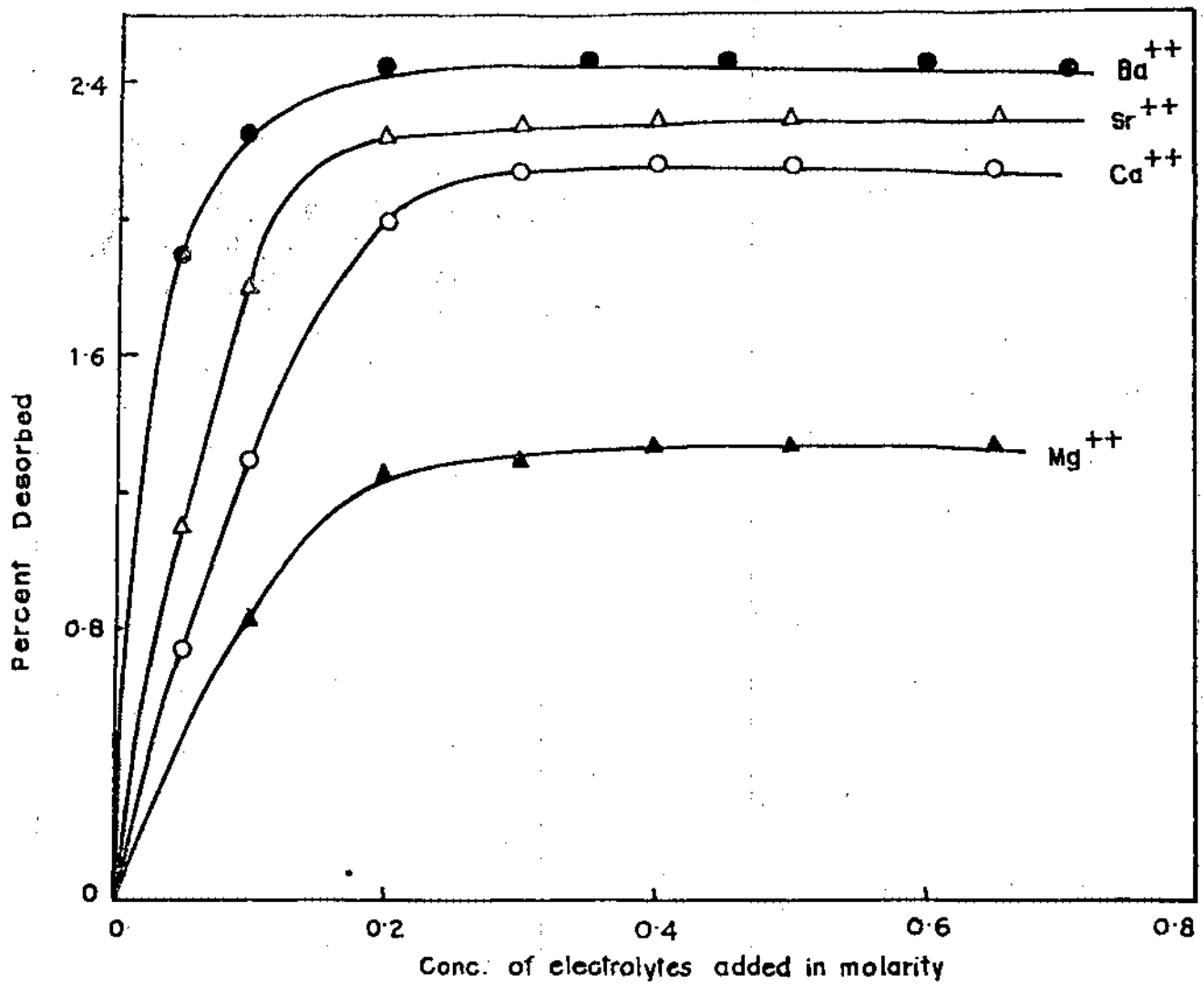

FIG. 100. DESORPTION OF METHYLENE BLUE FROM Na- MONTMORILLONITE BY VARIOUS DIVALENT IONS.

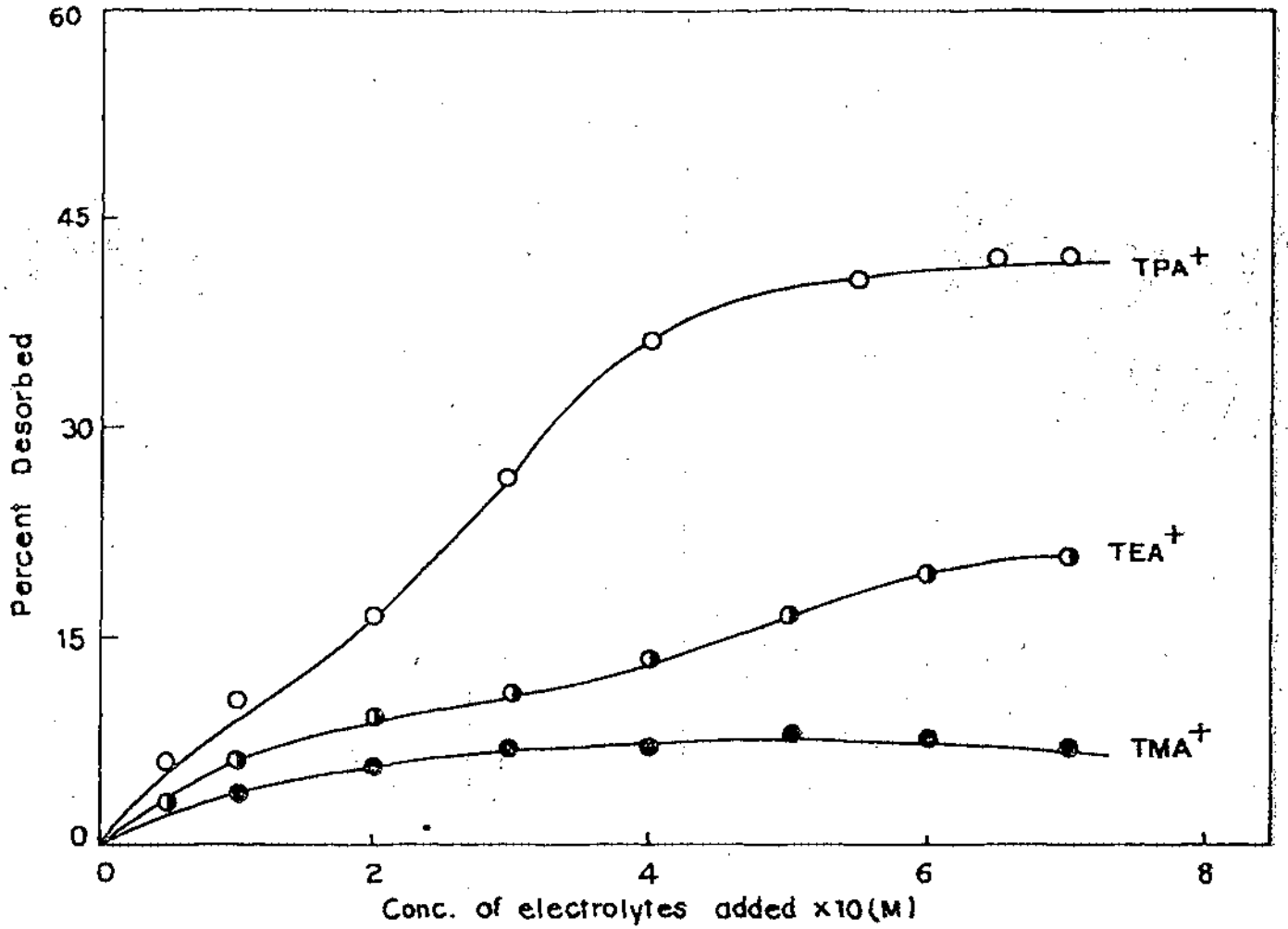

FIG. 101 DESORPTION OF METHYLENE BLUE FROM Na-MONTMORILLONITE BY VARIOUS TETRA-ALKYL AMMONIUM IONS.

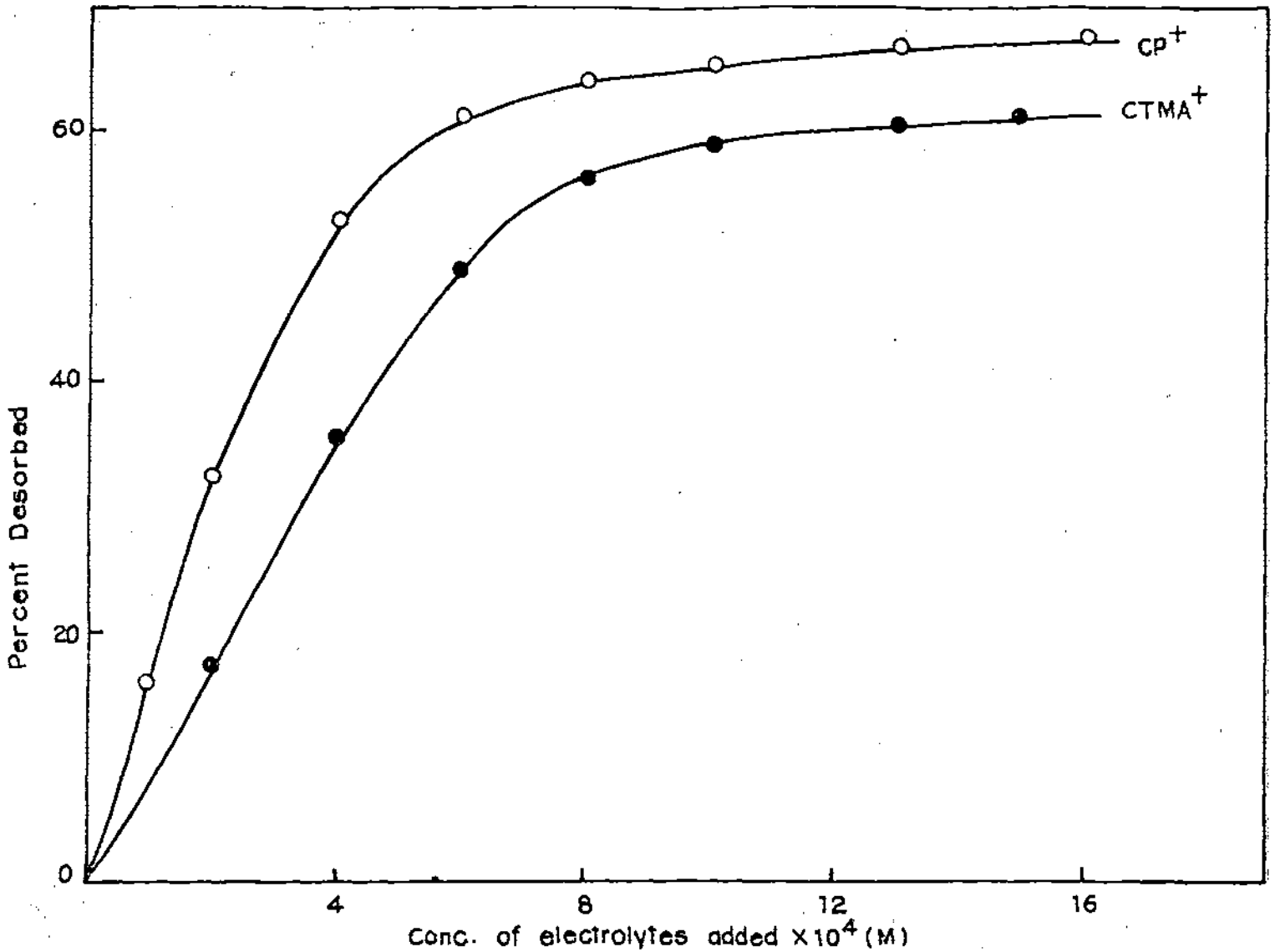

FIG. 102 DESORPTION OF METHYLENE BLUE FROM Na-MONTMORILLONITE BY LONG CHAIN SURFACE ACTIVE TRIMETHYL AMMONIUM AND PYRIDINIUM IONS.

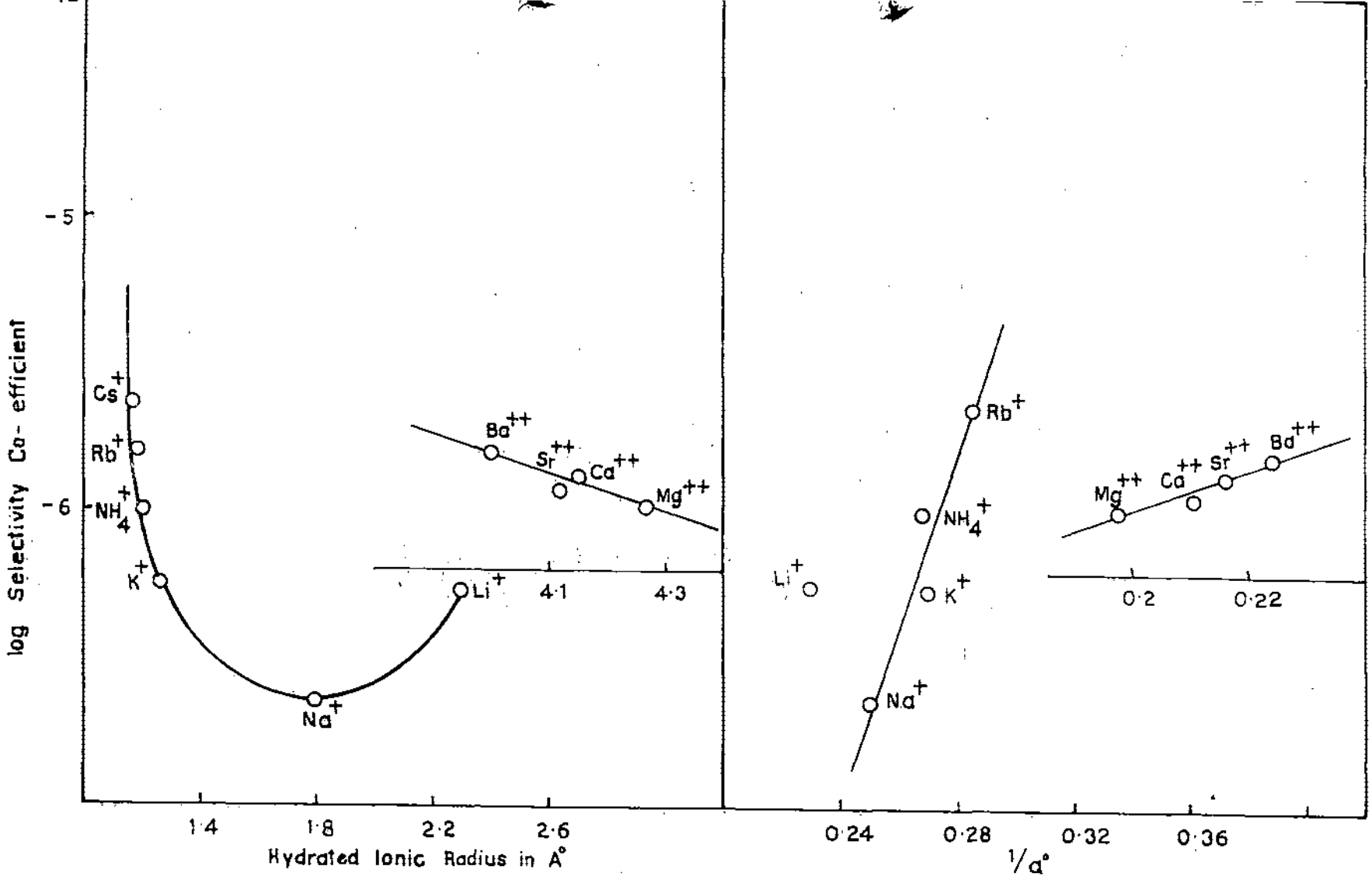

FIG. 103. CORRELATION OF SELECTIVITY CO-EFFICIENT WITH HYDRATED IONIC RADIUS AND DEBYE-HUCKEL PARAMETER a° IN THE DESORPTION OF MMT (AZURE-C) FROM Na-MONTMORILLONITE-MMT.

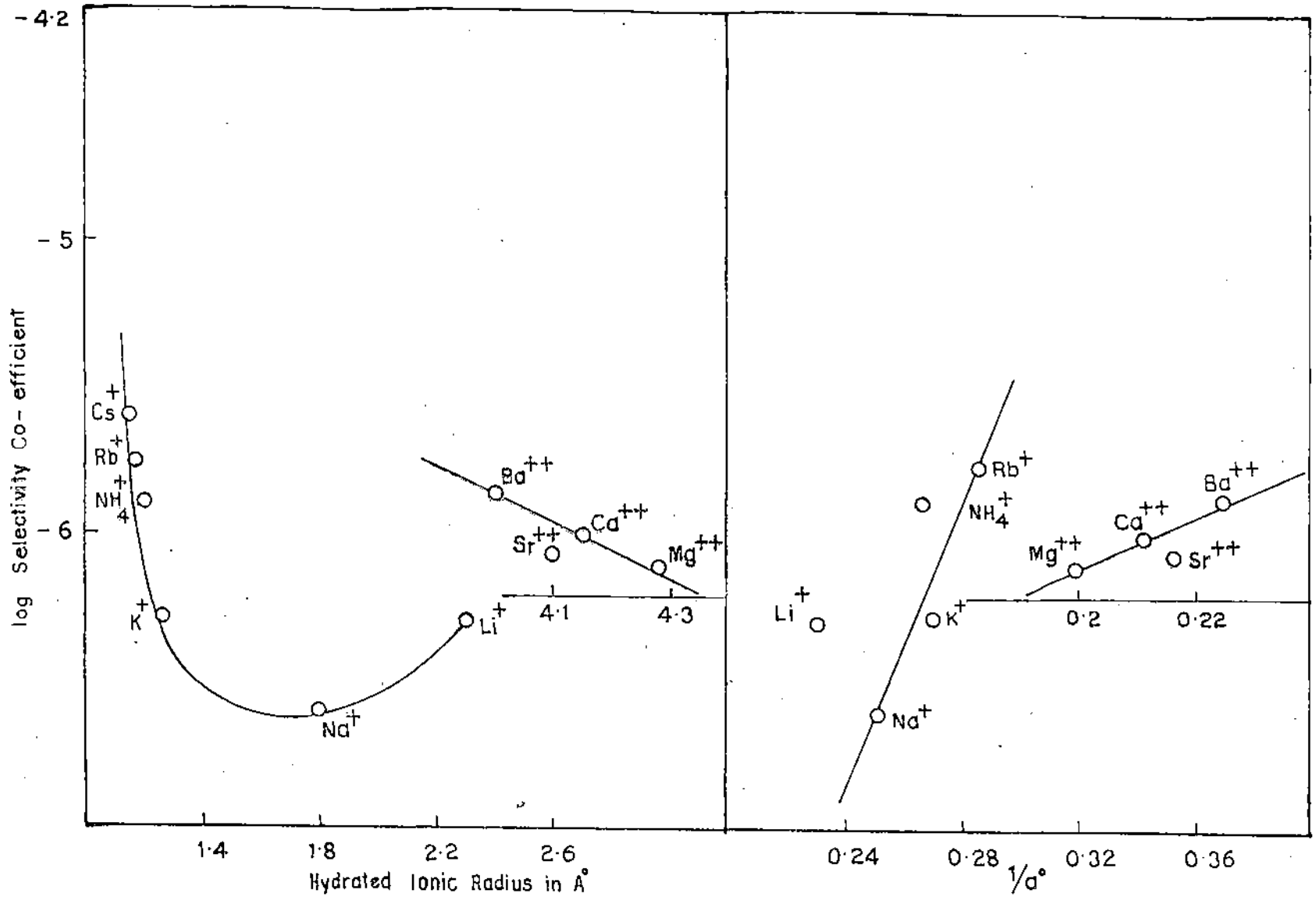

FIG. 104. CORRELATION OF SELECTIVITY COEFFICIENT WITH HYDRATED IONIC RADIUS AND DEBYE-HUCKEL PARAMETER a°, IN THE DESORPTION OF DMT (AZURE-A) FROM Na-MONTMORILLONITE-DMT.

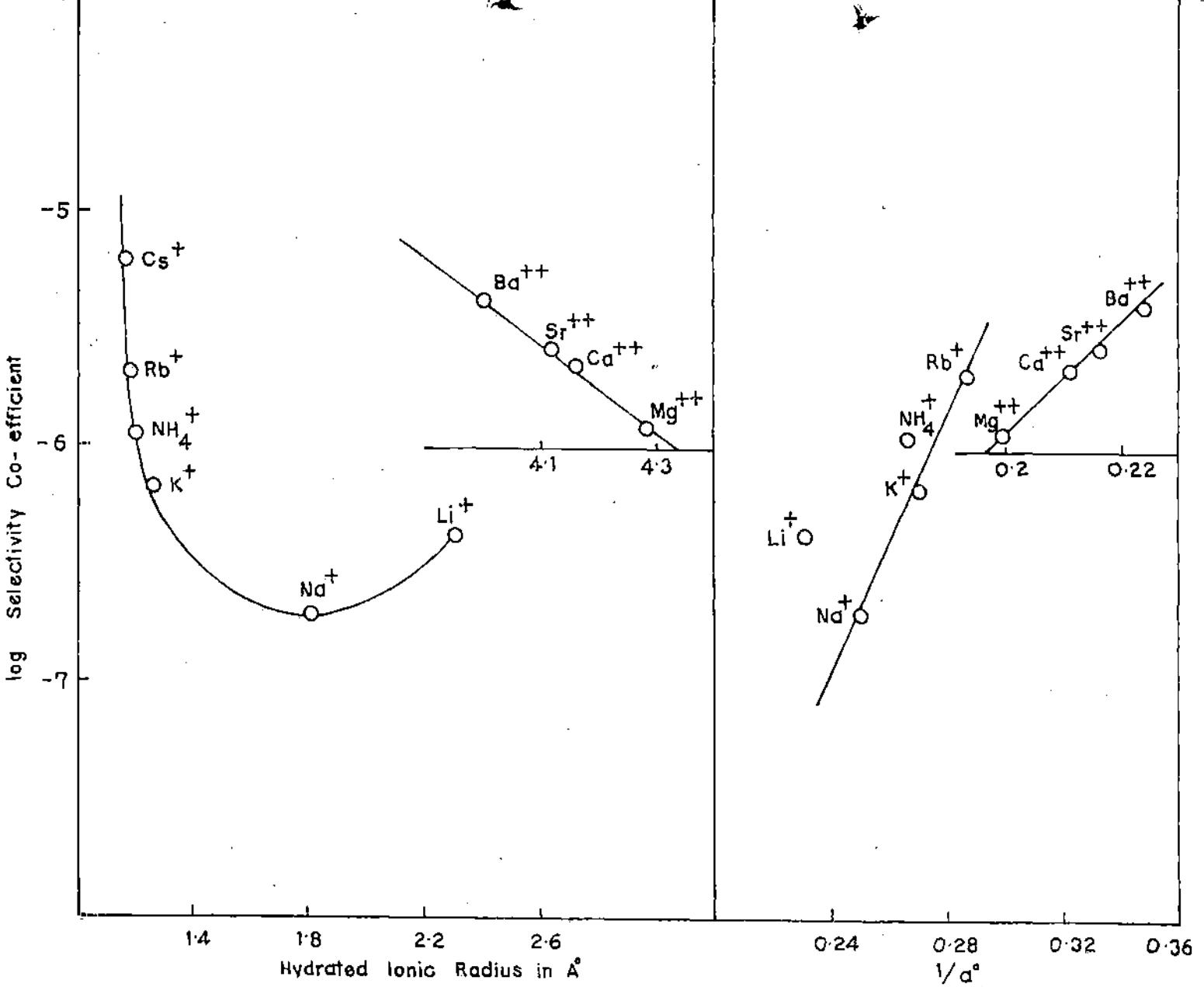

FIG. 105 CORRELATION OF SELECTIVITY COEFFICIENT WITH HYDRATED IONIC RADIUS AND DEBYE-HUCKEL PARAMETER a° IN THE DESORPTION OF TMT (AZURE-B) FROM Na-MONTMORILLONITE - TMT.

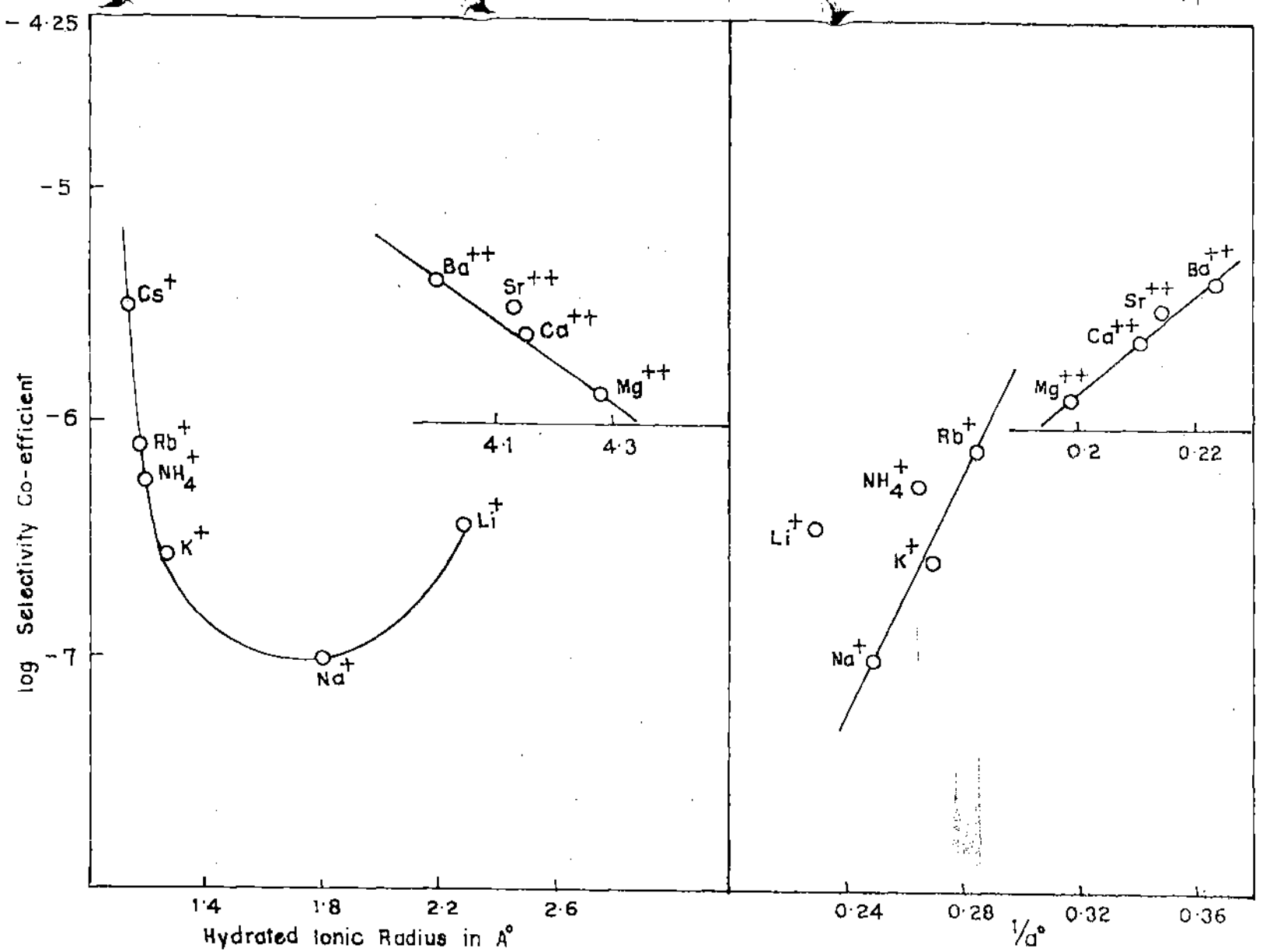

FIG. 106 CORRELATION OF SELECTIVITY COEFFICIENT WITH HYDRATED IONIC RADIUS AND DEBYE-HUCKEL PARAMETER a° IN THE DESORPTION OF METHYLENE BLUE FROM Na-MONTMORILLONITE-MB.

Table - 23

Desorption characteristics of Thionine from Na-Montmorillonite-Thionine with respect to different ions

Electrolyte used	Concentration of Electrolyte	Distribution Co-efficient	Selectivity Co-efficient
1:1 Electrolytes			
	0.10(M)	0.115	5.43×10^{-7}
LiCl	0.20(M)	0.090	6.69×10^{-7}
	0.30(M)	0.073	6.69×10^{-7}
	0.40(M)	0.065	7.04×10^{-7}
	0.50(M)	0.056	6.54×10^{-7}
	0.75(M)	0.040	5.02×10^{-7}
	0.10(M)	0.095	3.69×10^{-7}
NaCl	0.20(M)	0.070	4.03×10^{-7}
	0.30(M)	0.055	3.74×10^{-7}
	0.40(M)	0.045	3.34×10^{-7}
	0.50(M)	0.038	2.99×10^{-7}
	0.75(M)	0.027	2.32×10^{-7}
	0.10(M)	0.145	8.65×10^{-7}
KCl	0.20(M)	0.100	8.28×10^{-7}
	0.30(M)	0.083	8.67×10^{-7}
	0.40(M)	0.063	6.77×10^{-7}
	0.50(M)	0.053	5.85×10^{-7}
	0.75(M)	0.040	5.02×10^{-7}
	0.10(M)	0.180	1.34×10^{-6}
NH_4Cl	0.20(M)	0.128	1.35×10^{-6}
	0.30(M)	0.112	1.57×10^{-6}
	0.40(M)	0.086	1.25×10^{-6}
	0.50(M)	0.073	1.12×10^{-6}
	0.75(M)	0.053	9.03×10^{-7}

Contd..

Electrolyte used	Concentration of Electrolyte	Distribution Co-efficient	Selectivity Co-efficient
	0.10(M)	0.225	2.10×10^{-6}
RbCl	0.20(M)	0.165	2.29×10^{-6}
	0.30(M)	0.135	2.31×10^{-6}
	0.40(M)	0.116	2.41×10^{-6}
	0.50(M)	0.107	2.46×10^{-6}
	0.75(M)	0.083	2.26×10^{-6}
	0.10(M)	0.275	3.16×10^{-6}
CsCl	0.20(M)	0.215	3.92×10^{-6}
	0.30(M)	0.182	4.25×10^{-6}
	0.40(M)	0.156	4.23×10^{-6}
	0.50(M)	0.135	3.97×10^{-6}
	0.75(M)	0.100	3.29×10^{-6}
2:1 Electrolyte			
	0.05(M)	0.609	4.69×10^{-6}
	0.10(M)	0.514	5.69×10^{-6}
$BaCl_2$	0.20(M)	0.418	6.16×10^{-6}
	0.30(M)	0.358	5.85×10^{-6}
	0.40(M)	0.323	5.61×10^{-6}
	0.50(M)	0.288	5.07×10^{-6}
	0.05(M)	0.521	2.92×10^{-6}
$SrCl_2$	0.10(M)	0.475	4.46×10^{-6}
	0.20(M)	0.398	5.32×10^{-6}
	0.30(M)	0.347	5.32×10^{-6}
	0.40(M)	0.312	5.17×10^{-6}
	0.50(M)	0.288	5.07×10^{-6}

Contd..

Electrolyte used	Concentration of Electrolyte	Distribution Co-efficient	Selectivity Co-efficient
	0.05(M)	0.489	2.42×10^{-6}
	0.10(M)	0.447	3.71×10^{-6}
$CaCl_2$	0.20(M)	0.387	4.86×10^{-6}
	0.30(M)	0.348	5.37×10^{-6}
	0.40(M)	0.312	5.17×10^{-6}
	0.50(M)	0.282	4.75×10^{-6}
	0.05(M)	0.447	1.83×10^{-6}
	0.10(M)	0.414	2.92×10^{-6}
$MgCl_2$	0.20(M)	0.366	4.09×10^{-6}
	0.30(M)	0.329	4.47×10^{-6}
	0.40(M)	0.302	4.65×10^{-6}
	0.50(M)	0.277	4.44×10^{-6}
Quartemary Ammonium Salt			
	0.05(M)	0.509	5.21×10^{-6}
	0.10(M)	0.501	1.07×10^{-5}
TMABr	0.20(M)	0.400	1.41×10^{-5}
	0.30(M)	0.367	1.84×10^{-5}
	0.40(M)	0.338	2.15×10^{-5}
	0.50(M)	0.300	2.16×10^{-5}
	0.05(M)	0.900	1.72×10^{-5}
	0.10(M)	0.850	3.21×10^{-5}
TEABr	0.20(M)	0.900	8.06×10^{-5}
	0.30(M)	0.867	1.25×10^{-4}
	0.40(M)	0.775	1.43×10^{-4}
	0.50(M)	0.670	1.39×10^{-4}

Contd..

Electrolyte used	Concentration of Electrolyte	Distribution Co-efficient	Selectivity Co-efficient
	0.05(M)	1.600	5.66×10^{-5}
	0.10(M)	1.400	9.28×10^{-5}
TPABr	0.20(M)	1.225	1.63×10^{-4}
	0.30(M)	1.117	2.31×10^{-4}
	0.40(M)	0.988	2.66×10^{-4}
	0.50(M)	0.850	2.59×10^{-4}
	2.0×10^{-4}(M)	649.014	0.034
	4.0×10^{-4}(M)	846.756	0.141
CTMABr	6.0×10^{-4}(M)	801.635	0.234
	8.0×10^{-4}(M)	729.770	0.315
	1.0×10^{-3}(M)	687.493	0.442
	1.2×10^{-3}(M)	575.655	0.395
	2.0×10^{-4}(M)	1208.740	0.119
CPBr	4.0×10^{-4}(M)	1058.734	0.234
	6.0×10^{-4}(M)	927.418	0.340
	8.0×10^{-4}(M)	838.243	0.474
	1.0×10^{-4}(M)	726.496	0.534
	1.2×10^{-4}(M)	633.134	0.560

Table - 24

Desorption characteristics of MMT(Azure-C) from Na-Montmorillonite-MMT with respect to different ions

Electrolyte used	Concentration of Electrolytes	Distribution Coefficient	Selectivity Co-efficient
1:1 Electrolyte			
	0.10(M)	0.065	2.99×10^{-7}
LiCl	0.20(M)	0.080	6.11×10^{-7}
	0.30(M)	0.068	6.72×10^{-7}
	0.40(M)	0.060	6.93×10^{-7}
	0.50(M)	0.052	6.52×10^{-7}
	0.75(M)	0.036	4.87×10^{-7}
	0.10(M)	0.055	1.42×10^{-7}
NaCl	0.20(M)	0.052	2.61×10^{-7}
	0.30(M)	0.043	2.67×10^{-7}
	0.40(M)	0.037	2.68×10^{-7}
	0.50(M)	0.034	2.76×10^{-7}
	0.75(M)	0.023	1.95×10^{-7}
	0.10(M)	0.090	3.83×10^{-7}
KCl	0.20(M)	0.075	5.36×10^{-7}
	0.30(M)	0.065	6.07×10^{-7}
	0.40(M)	0.057	6.36×10^{-7}
	0.50(M)	0.052	6.52×10^{-7}
	0.75(M)	0.040	5.82×10^{-7}
	0.10(M)	0.125	7.42×10^{-7}
NH_4Cl	0.20(M)	0.097	9.11×10^{-7}
	0.30(M)	0.083	1.00×10^{-6}
	0.40(M)	0.073	1.05×10^{-6}
	0.50(M)	0.066	1.06×10^{-6}
	0.75(M)	0.051	9.73×10^{-7}

Contd..

Electrolyte used	Concentration of Electrolyte	Distribution Co-efficient	Selectivity Co-efficient
	0.10(M)	0.150	1.07×10^{-6}
RbCl	0.20(M)	0.120	1.38×10^{-6}
	0.30(M)	0.108	1.71×10^{-6}
	0.40(M)	0.098	1.91×10^{-6}
	0.50(M)	0.092	2.09×10^{-6}
	0.75(M)	0.078	2.25×10^{-6}
	0.10(M)	0.185	1.63×10^{-6}
CsCl	0.20(M)	0.142	1.93×10^{-6}
	0.30(M)	0.121	2.17×10^{-6}
	0.40(M)	0.112	2.50×10^{-6}
	0.50(M)	0.102	2.58×10^{-6}
	0.75(M)	0.085	2.76×10^{-6}
2:1 Electrolyte			
	0.05(M)	0.250	1.48×10^{-6}
$BaCl_2$	0.10(M)	0.185	1.63×10^{-6}
	0.20(M)	0.135	1.76×10^{-6}
	0.30(M)	0.106	1.66×10^{-6}
	0.40(M)	0.086	1.45×10^{-6}
	0.50(M)	0.072	1.26×10^{-6}
	0.05(M)	0.225	1.20×10^{-6}
	0.10(M)	0.182	1.59×10^{-6}
$SrCl_2$	0.20(M)	0.135	1.76×10^{-6}
	0.30(M)	0.094	1.28×10^{-6}
	0.40(M)	0.080	1.24×10^{-6}
	0.50(M)	0.066	1.06×10^{-6}

Contd..

Electrolyte used	Concentration of Electrolyte	Distribution Co-efficient	Selectivity Co-efficient
	0.05 (M)	0.182	7.84×10^{-7}
$CaCl_2$	0.10 (M)	0.175	1.46×10^{-6}
	0.20 (M)	0.122	1.44×10^{-6}
	0.30 (M)	0.091	1.21×10^{-6}
	0.40 (M)	0.075	1.09×10^{-6}
	0.50 (M)	0.063	9.64×10^{-7}
	0.05 (M)	0.165	6.43×10^{-7}
$MgCl_2$	0.10 (M)	0.100	4.74×10^{-7}
	0.20 (M)	0.101	9.83×10^{-7}
	0.30 (M)	0.070	7.05×10^{-7}
	0.40 (M)	0.058	6.52×10^{-7}
	0.50 (M)	0.051	6.27×10^{-7}
Quarternary Ammonium Salt			
	0.05 (M)	0.400	3.83×10^{-6}
TMABr	0.10 (M)	0.301	4.36×10^{-6}
	0.20 (M)	0.321	1.06×10^{-5}
	0.30 (M)	0.266	1.10×10^{-5}
	0.40 (M)	0.286	1.69×10^{-5}
	0.50 (M)	0.240	1.56×10^{-5}
	0.05 (M)	0.500	6.03×10^{-6}
TEABr	0.10 (M)	0.401	7.85×10^{-6}
	0.20 (M)	0.375	1.44×10^{-5}
	0.30 (M)	0.366	2.10×10^{-5}
	0.40 (M)	0.400	3.67×10^{-5}
	0.50 (M)	0.412	4.01×10^{-5}

Contd..

Electrolyte used	Concentration of Electrolyte	Distribution Co-efficient	Selectivity Co-efficient
	0.05(M)	1.300	4.27×10^{-5}
TPABr	0.10(M)	1.100	6.48×10^{-5}
	0.20(M)	0.901	9.55×10^{-5}
	0.30(M)	0.800	1.24×10^{-4}
	0.40(M)	0.775	1.74×10^{-4}
	0.50(M)	0.781	2.51×10^{-4}
	2.0×10^{-4}(M)	783.400	0.058
CTMABr	4.0×10^{-4}(M)	716.841	0.117
	6.0×10^{-4}(M)	662.560	0.181
	8.0×10^{-4}(M)	549.350	0.185
	1.0×10^{-3}(M)	619.891	0.330
	1.2×10^{-3}(M)	609.321	0.422
	2.0×10^{-4}(M	1420.270	0.195
	4.0×10^{-4}(M)	1160.540	0.356
CPBr	6.0×10^{-4}(M)	1005.020	0.549
	8.0×10^{-4}(M)	868.860	0.737
	1.0×10^{-3}(M)	776.671	1.041
	1.2×10^{-3}(M)	711.360	1.672

Table - 25

Desorption characteristics of DMT (Azure-A) from Na-Montmorillonite-DMT with respect to different ions

Electrolyte used	Concentration of Electrolyte	Distribution Co-efficient	Selectivity Co-efficient
1:1 Electrolyte			
	0.10(M)	0.085	3.98×10^{-7}
	0.20(M)	0.075	6.26×10^{-7}
LiCl	0.30(M)	0.066	7.31×10^{-7}
	0.40(M)	0.055	6.79×10^{-7}
	0.50(M)	0.490	6.76×10^{-7}
	0.75(M)	0.033	4.69×10^{-7}
	0.10(M)	0.055	1.66×10^{-7}
NaCl	0.20(M)	0.052	3.05×10^{-7}
	0.30(M)	0.045	3.37×10^{-7}
	0.40(M)	0.034	2.53×10^{-7}
	0.50(M)	0.031	2.68×10^{-7}
	0.75(M)	0.020	1.67×10^{-7}
	0.10(M)	0.075	3.09×10^{-7}
	0.20(M)	0.065	4.69×10^{-7}
KCl	0.30(M)	0.058	5.69×10^{-7}
	0.40(M)	0.052	6.18×10^{-7}
	0.50(M)	0.045	5.69×10^{-7}
	0.75(M)	0.034	5.08×10^{-7}
	0.10(M)	0.125	8.66×10^{-7}
	0.20(M)	0.105	1.24×10^{-6}
NH_4Cl	0.30(M)	0.092	1.43×10^{-6}
	0.40(M)	0.080	1.46×10^{-6}
	0.50(M)	0.069	1.39×10^{-6}
	0.75(M)	0.049	1.07×10^{-6}

Contd..

Electrolyte used	Concentration of Electrolyte	Distribution Co-efficient	Selectivity Co-efficient
	0.10(M)	0.145	1.17×10^{-6}
	0.20(M)	0.118	1.55×10^{-6}
RbCl	0.30(M)	0.103	1.82×10^{-6}
	0.40(M)	0.094	2.02×10^{-6}
	0.50(M)	0.085	2.09×10^{-6}
	0.75(M)	0.065	1.86×10^{-6}
	0.10(M)	0.175	1.71×10^{-6}
	0.20(M)	0.148	2.47×10^{-6}
CsCl	0.30(M)	0.123	2.61×10^{-6}
	0.40(M)	0.113	2.93×10^{-6}
	0.50(M)	0.102	3.04×10^{-6}
	0.75(M)	0.077	2.59×10^{-6}
2:1 Electrolyte			
	0.05(M)	0.220	1.33×10^{-6}
	0.10(M)	0.178	1.76×10^{-6}
$BaCl_2$	0.20(M)	0.126	1.79×10^{-6}
	0.30(M)	0.076	1.20×10^{-6}
	0.40(M)	0.075	1.27×10^{-6}
	0.50(M)	0.060	1.02×10^{-6}
	0.05(M)	0.150	6.19×10^{-7}
$SrCl_2$	0.10(M)	0.125	8.66×10^{-7}
	0.20(M)	0.105	1.23×10^{-6}
	0.30(M)	0.086	1.26×10^{-6}
	0.40(M)	0.068	1.05×10^{-6}
	0.50(M)	0.056	8.87×10^{-7}

Contd..

Electrolyte used	Concentration of Electrolyte	Distribution Co-efficient	Selectivity Co-efficient
	0.05(M)	0.110	3.32×10^{-7}
	0.10(M)	0.100	5.52×10^{-7}
$CaCl_2$	0.20(M)	0.087	8.44×10^{-7}
	0.30(M)	0.083	1.16×10^{-6}
	0.40(M)	0.058	7.66×10^{-7}
	0.50(M)	0.053	7.93×10^{-7}
	0.05(M)	0.090	2.22×10^{-7}
	0.10(M)	0.075	3.09×10^{-7}
$MgCl_2$	0.20(M)	0.067	5.02×10^{-7}
	0.30(M)	0.059	5.83×10^{-7}
	0.40(M)	0.048	5.23×10^{-7}
	0.50(M)	0.042	4.94×10^{-7}
Quarternary Ammonium Salt			
	0.05(M)	0.300	2.50×10^{-6}
	0.10(M)	0.201	2.24×10^{-6}
TMABr	0.20(M)	0.200	4.60×10^{-6}
	0.30(M)	0.200	7.10×10^{-6}
	0.40(M)	0.187	8.48×10^{-6}
	0.50(M)	0.180	1.00×10^{-5}
	0.05(M)	0.400	4.48×10^{-6}
	0.10(M)	0.351	7.00×10^{-6}
TEABr	0.20(M)	0.350	1.47×10^{-5}
	0.30(M)	0.350	2.32×10^{-5}
	0.40(M)	0.375	3.81×10^{-5}
	0.50(M)	0.390	5.76×10^{-5}

Contd..

Electrolyte used	Concentration of Electrolyte	Distribution Co-efficient	Selectivity Co-efficient
	0.05(M)	1.200	4.26×10^{-5}
	0.10(M)	1.050	6.97×10^{-5}
TPABr	0.20(M)	0.925	1.23×10^{-4}
	0.30(M)	0.766	1.37×10^{-4}
	0.40(M)	0.700	1.68×10^{-4}
	0.50(M)	0.740	2.39×10^{-4}
	2.0×10^{-4}(M)	718.562	0.058
CTMABr	4.0×10^{-4}(M)	605.278	0.098
	6.0×10^{-4}(M)	578.988	0.164
	8.0×10^{-4}(M)	558.139	0.255
	1.0×10^{-3}(M)	545.707	0.406
	1.2×10^{-3}(M)	532.304	0.674
	2.0×10^{-4}(M)	1344.000	0.212
CPBr	4.0×10^{-4}(M)	1088.817	0.393
	6.0×10^{-4}(M)	936.099	0.623
	8.0×10^{-4}(M)	819.512	0.937
	1.0×10^{-3}(M)	718.562	1.346
	1.2×10^{-3}(M)	637.168	2.013

Table - 26

Desorption characteristics of TMT (Azure-B) from Na-Montmorillonite - TMT with respect to different ions

Electrolyte used	Concentration of Electrolytes	Distribution Co-efficient	Selectivity Co-efficient
1:1 Electrolyte			
	0.10(M)	0.070	3.00×10^{-7}
	0.20(M)	0.052	3.36×10^{-7}
LiCl	0.30(M)	0.050	4.65×10^{-7}
	0.40(M)	0.043	4.68×10^{-7}
	0.50(M)	0.040	4.99×10^{-7}
	0.75(M)	0.029	4.00×10^{-7}
	0.10(M)	0.020	9.48×10^{-8}
NaCl	0.20(M)	0.032	1.29×10^{-7}
	0.30(M)	0.027	1.56×10^{-7}
	0.40(M)	0.025	1.53×10^{-7}
	0.50(M)	0.024	1.77×10^{-7}
	0.75(M)	0.016	1.18×10^{-7}
	0.10(M)	0.075	3.45×10^{-7}
	0.20(M)	0.062	4.82×10^{-7}
KCl	0.30(M)	0.058	6.31×10^{-7}
	0.40(M)	0.052	6.83×10^{-7}
	0.50(M)	0.047	6.93×10^{-7}
	0.75(M)	0.033	5.19×10^{-7}
	0.10(M)	0.120	8.89×10^{-7}
NH_4Cl	0.20(M)	0.097	1.18×10^{-6}
	0.30(M)	0.083	1.30×10^{-6}
	0.40(M)	0.071	1.28×10^{-6}
	0.50(M)	0.062	1.22×10^{-6}
	0.75(M)	0.042	8.54×10^{-7}

Contd..

Electrolyte used	Concentration of Electrolyte	Distribution Co-efficient	Selectivity Co-efficient
	0.10(M)	0.160	1.58×10^{-6}
	0.20(M)	0.130	2.13×10^{-6}
RbCl	0.30(M)	0.113	2.45×10^{-6}
	0.40(M)	0.093	2.23×10^{-6}
	0.50(M)	0.084	2.27×10^{-6}
	0.75(M)	0.060	1.75×10^{-6}
	0.10(M)	0.220	3.03×10^{-6}
	0.20(M)	0.174	3.86×10^{-6}
CsCl	0.30(M)	0.141	3.87×10^{-6}
	0.40(M)	0.122	3.90×10^{-6}
	0.50(M)	0.098	3.98×10^{-6}
	0.75(M)	0.078	3.81×10^{-6}
2:1 Electrolyte			
	0.05(M)	0.200	1.23×10^{-6}
	0.10(M)	0.172	1.84×10^{-6}
$BaCl_2$	0.20(M)	0.130	2.13×10^{-6}
	0.30(M)	0.094	1.67×10^{-6}
	0.40(M)	0.071	1.28×10^{-6}
	0.50(M)	0.057	1.03×10^{-6}
	0.05(M)	0.150	9.10×10^{-7}
	0.10(M)	0.127	1.00×10^{-6}
$SrCl_2$	0.20(M)	0.098	1.21×10^{-6}
	0.30(M)	0.074	1.11×10^{-6}
	0.40(M)	0.064	1.03×10^{-6}
	0.50(M)	0.051	9.88×10^{-7}

Contd..

Electrolyte used	Concentration of Electrolyte	Distribution Co-efficient	Selectivity Co-efficient
	0.05(M)	0.110	8.70×10^{-7}
	0.10(M)	0.100	1.03×10^{-6}
$CaCl_2$	0.20(M)	0.093	1.21×10^{-6}
	0.30(M)	0.081	1.24×10^{-6}
	0.40(M)	0.064	1.03×10^{-6}
	0.50(M)	0.051	9.98×10^{-7}
	0.05(M)	0.065	1.28×10^{-7}
	0.10(M)	0.064	2.94×10^{-7}
$MgCl_2$	0.20(M)	0.060	4.91×10^{-7}
	0.30(M)	0.060	6.80×10^{-7}
	0.40(M)	0.050	6.24×10^{-7}
	0.50(M)	0.045	4.98×10^{-7}
Quarternary Ammoniumt Salt	0.05(M)	0.250	1.93×10^{-6}
	0.10(M)	0.230	4.31×10^{-6}
TMABr	0.20(M)	0.215	6.12×10^{-6}
	0.30(M)	0.201	8.07×10^{-6}
	0.40(M)	0.191	9.18×10^{-6}
	0.50(M)	0.180	1.12×10^{-5}
	0.05(M)	0.400	4.99×10^{-6}
	0.10(M)	0.369	8.98×10^{-6}
TEABr	0.20(M)	0.375	1.91×10^{-5}
	0.30(M)	0.374	2.51×10^{-5}
	0.40(M)	0.371	4.12×10^{-5}
	0.50(M)	0.370	4.84×10^{-5}

Contd..

Electrolyte used	Concentration of Electrolyte	Distribution Co-efficient	Selectivity Co-efficient
	0.05(M)	0.800	2.05×10^{-5}
	0.10(M)	0.750	3.82×10^{-5}
TPABr	0.20(M)	0.641	8.31×10^{-5}
	0.30(M)	0.660	1.29×10^{-4}
	0.40(M)	0.661	1.59×10^{-4}
	0.50(M)	0.660	2.49×10^{-4}
	2.0×10^{-4}(M)	704.56	0.063
	4.0×10^{-4}(M)	650.18	0.183
CTMABr	6.0×10^{-4}(M)	612.43	0.224
	8.0×10^{-4}(M)	565.32	0.397
	1.0×10^{-3}(M)	525.41	0.663
	1.2×10^{-3}(M)	499.82	0.715
	2.0×10^{-4}(M)	1053.23	0.145
	4.0×10^{-4}(M)	955.12	0.398
CPBr	6.0×10^{-4}(M)	834.42	0.542
	8.0×10^{-4}(M)	786.31	0.987
	1.0×10^{-3}(M)	631.25	2.109
	1.2×10^{-3}(M)	612.43	3.204

Table - 27

Desorption characteristics of Methylene Blue from Na-Montmorillonite-MB with respect to different ions

Electrolyte used	Concentration of Electrolytes	Distribution Co-efficient	Selectivity Co-efficient
1:1 Electrolyte			
	0.10(M)	0.095	5.93×10^{-7}
	0.20(M)	0.060	4.75×10^{-7}
LiCl	0.30(M)	0.041	3.39×10^{-7}
	0.40(M)	0.033	2.89×10^{-7}
	0.50(M)	0.029	2.81×10^{-7}
	0.75(M)	0.019	1.83×10^{-7}
	0.10(M)	0.049	1.58×10^{-7}
NaCl	0.20(M)	0.037	1.81×10^{-7}
	0.30(M)	0.031	1.93×10^{-7}
	0.40(M)	0.025	1.64×10^{-7}
	0.50(M)	0.020	1.34×10^{-7}
	0.75(M)	0.013	9.98×10^{-8}
	0.10(M)	0.070	3.20×10^{-7}
KCl	0.20(M)	0.041	2.21×10^{-7}
	0.30(M)	0.034	2.36×10^{-7}
	0.40(M)	0.035	2.43×10^{-7}
	0.50(M)	0.022	1.63×10^{-7}
	0.75(M)	0.015	1.11×10^{-7}
	0.10(M)	0.105	7.25×10^{-7}
NH_4Cl	0.20(M)	0.064	5.41×10^{-7}
	0.30(M)	0.049	6.83×10^{-7}
	0.40(M)	0.038	1.83×10^{-6}
	0.50(M)	0.028	4.21×10^{-7}
	0.75(M)	0.020	6.05×10^{-7}

Contd..

Electrolyte used	Concentration of Electrolyte	Distribution Co-efficient	Selectivity Co-efficient
	0.10(M)	0.128	1.08×10^{-6}
	0.20(M)	0.087	1.01×10^{-6}
RbCl	0.30(M)	0.066	8.81×10^{-7}
	0.40(M)	0.058	7.81×10^{-7}
	0.50(M)	0.044	6.48×10^{-7}
	0.75(M)	0.033	6.98×10^{-7}
	0.10(M)	0.205	2.80×10^{-6}
	0.20(M)	0.127	2.17×10^{-6}
CsCl	0.30(M)	0.091	1.68×10^{-6}
	0.40(M)	0.073	2.01×10^{-6}
	0.50(M)	0.058	1.84×10^{-6}
	0.75(M)	0.049	8.89×10^{-7}
2:1 Electrolyte	0.05(M)	0.380	3.42×10^{-6}
	0.10(M)	0.220	3.24×10^{-6}
$BaCl_2$	0.20(M)	0.120	1.93×10^{-6}
	0.30(M)	0.095	1.85×10^{-6}
	0.40(M)	0.062	1.02×10^{-6}
	0.50(M)	0.048	7.80×10^{-7}
	0.05(M)	0.260	2.23×10^{-6}
	0.10(M)	0.183	2.11×10^{-6}
$SrCl_2$	0.20(M)	0.110	1.62×10^{-6}
	0.30(M)	0.089	1.01×10^{-6}
	0.40(M)	0.057	8.79×10^{-7}
	0.50(M)	0.043	7.89×10^{-7}

Contd..

Electrolyte used	Concentration of Electrolyte	Distribution Co-efficient	Selectivity Co-efficient
	0.05(M)	0.144	6.79×10^{-7}
	0.10(M)	0.130	1.11×10^{-6}
$CaCl_2$	0.20(M)	0.091	1.01×10^{-6}
	0.30(M)	0.070	9.82×10^{-7}
	0.40(M)	0.057	8.71×10^{-7}
	0.50(M)	0.045	7.91×10^{-7}
	0.05(M)	0.100	3.26×10^{-7}
	0.10(M)	0.080	4.19×10^{-7}
$MgCl_2$	0.20(M)	0.062	5.07×10^{-7}
	0.30(M)	0.043	3.69×10^{-7}
	0.40(M)	0.033	2.94×10^{-7}
	0.50(M)	0.027	2.42×10^{-7}
Quarternary Ammonium Salt			
	0.05(M)	0.450	7.53×10^{-6}
	0.10(M)	0.351	8.78×10^{-6}
TMABr	0.20(M)	0.297	1.25×10^{-5}
	0.30(M)	0.221	1.13×10^{-5}
	0.40(M)	0.189	9.50×10^{-6}
	0.50(M)	0.158	8.51×10^{-6}
	0.05(M)	0.669	1.57×10^{-5}
TEABr	0.10(M)	0.602	2.58×10^{-5}
	0.20(M)	0.445	2.94×10^{-5}
	0.30(M)	0.350	2.89×10^{-5}
	0.40(M)	0.321	3.91×10^{-5}
	0.50(M)	0.330	4.60×10^{-5}

Contd..

Electrolyte used	Concentration of Electrolyte	Distribution Co-efficient	Selectivity Co-efficient
	0.05(M)	1.100	9.26×10^{-5}
	0.10(M)	1.000	7.57×10^{-5}
TPABr	0.20(M)	0.912	1.11×10^{-4}
	0.30(M)	0.901	2.89×10^{-4}
	0.40(M)	0.900	4.36×10^{-4}
	0.50(M)	0.800	4.71×10^{-4}
	2.0×10^{-4}(M)	1070.181	0.159
CTMABr	4.0×10^{-4}(M)	994.260	0.398
	6.0×10^{-4}(M)	963.241	0.440
	8.0×10^{-4}(M)	816.800	0.940
	1.0×10^{-3}(M)	693.641	1.221
	1.2×10^{-3}(M)	576.101	1.379
	2.0×10^{-4}(M)	2561.571	1.015
	4.0×10^{-4}(M)	1862.523	2.603
CPBr	6.0×10^{-4}(M)	1318.200	4.307
	8.0×10^{-4}(M)	966.331	4.680
	1.0×10^{-3}(M)	761.340	5.012
	1.2×10^{-3}(M)	627.671	5.062